Degree course in Structural Civil Engineering

NUMERICAL PREDICTION OF GROUND-BORN VIBRATIONS ON A BUILDING

Relator:

Prof. Cecilia Surace
Prof. Jean-Marc Battini

Author:

Tommaso Meinardi

Co-Relator:

Dott. Marco Civera
Dott. Abbas Zangeneh Kamali

Academic year 2022/2023

Abstract

When a building is constructed close to high-speed traffic infrastructure, the assessment of the level of vibration in those structures is relevant to guarantee safety and comfort. As long as the number of those buildings is continuously rising, is important to have a method to evaluate ground-born vibrations that require the lower computational time possible.

The primary objective of this study is to apply a simplified method for calculating ground-borne vibrations in building structures. This is achieved by breaking down the procedure into multiple steps, resulting in a significant reduction of the overall computational time of the entire process.

In pursuit of this objective, various Finite Element Method-Perfectly Matched Layer (FEM-PML) models have been developed. These models serve the purpose of calculating foundation impedance, determining foundation displacements under the influence of a unitary load simulating traffic, and providing a reference solution. The reference solution encompasses the entire soil domain with the superstructure and serves as a benchmark for result comparisons.

Then, as the simplified approach, the finite element model of the building was employed. incorporating the impedance at the bottom of the columns and applying the computed displacements as a base motion. This model was utilized to assess the vibration levels on the floors.

The analysis of the impedance and the foundations' displacements have been conducted by taking into count a frequency range from 0.1 to 30 Hz.

The eigenfrequencies of the building have been evaluated before and after the introduction of the impedance at the bottom of the column, to see how the presence of the soil impacts the building itself, but also to check that the peaks in the frequency of the final results describe properly the building behavior.

The velocities of the floors have finally been evaluated and compared to the ones obtained by running the model that represents the reference solution, to check the reliability of the method.

Contents

List of Figures

List of Tables

Chapter 1

Introduction

As the predictions on the world population growth state that in 2050 the number of people living on the planet will be around 10 billion and that the 70% of them will live in cities [13], the construction demand for new structures, such as houses, hospitals, schools, etc. will rise.
According to that, the cities will face an enlargement and new structures will be built in areas around the cities, normally characterized by the presence of railways or highways, which are a huge source of vibrations.
Those vibrations, called ground-borne vibrations, have to be taken into count when a new building is thought to be rising close to a vibration source, because, if their level is too high, they can bring discomfort and, in the worst cases, to safety problems.
Also, there is the possibility that, due to induced vibrations, some sensitive equipment, such as the ones used in the hospitals, can experience dysfunctions.
To avoid problems related to ground-born vibrations, is necessary to assess the vibration levels during the design phase of the building, to evaluate if countermeasures against this kind of problem has to be introduced.
Then is clear as, every time there is a change in the design of the building, a new calculation has to be performed.
As the stated problem is complicated, a model that takes into count both the soil and the superstructure with its foundation must be used. The largest is the plant dimension of the building, the greater will be the soil domain, which means the presence of a lot of degrees of freedom in the model, which is translated in a huge computational time.
Therefore, a way to reduce the time for studying this type of problem can be of practical

interest, because would allow to drastically decrease the computational time.

1.1 Aim of the work

The aim of this Master's thesis is to assess if a method to compute ground-born vibrations without computing the whole model can be performed in order to obtain reliable and cautionary results.
Considering two different cases, that differ just in the types of foundations under the building, the differences between the method object of analysis and the reference solution can be caught and analyzed, in order to understand which type of solution is better for each case.
To do this, for both cases of study, a coupled finite element - perfectly matched layer (FEM-PML) model of the soil and a single foundation has been created to compute the impedances of the foundation and, in a second time, the displacements of the foundation induced by a point load external to the soil domain (Figure 1.1(b)); those impedances and displacements have been introduced in a FEM model of a three-story building (Figure 1.1(c)) respectively as a set of springs and dashpots and as a base motion, to evaluate the velocities of the floor slabs due to ground born vibrations.
The obtained velocities have been compared to the ones obtained from a FEM-PML model of soil, foundation and building, that represent the reference solution (Figure 1.1(a)).

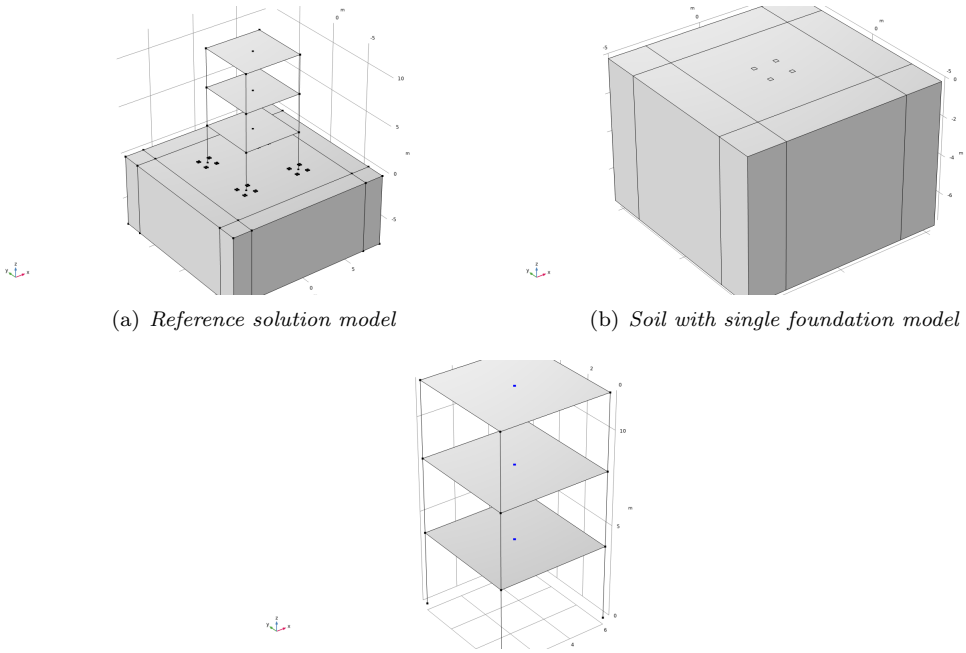

(a) *Reference solution model*

(b) *Soil with single foundation model*

(c) *Building model*

Figure 1.1: *FEM-PML model used to compute the reference solution (a), FEM-PML model with one foundation used to compute impedances and foundation's displacements (b), FEM model of the superstructure*

So then, the main goal of this thesis is to check that a method to assess groundborne vibrations that requires lower computational time is reliable enough to be used for practical purposes, for example, while designing a building close to a source of vibration as a railway or a highway can be.

1.2 Cases of study

The cases of study that have been taken into consideration for the following study are two: one considering the reference building on piles groups foundations and one considering the reference building on slab foundations.
They differ just in the type of foundation under the building, because the properties of the superstructure and of the soil are the same.

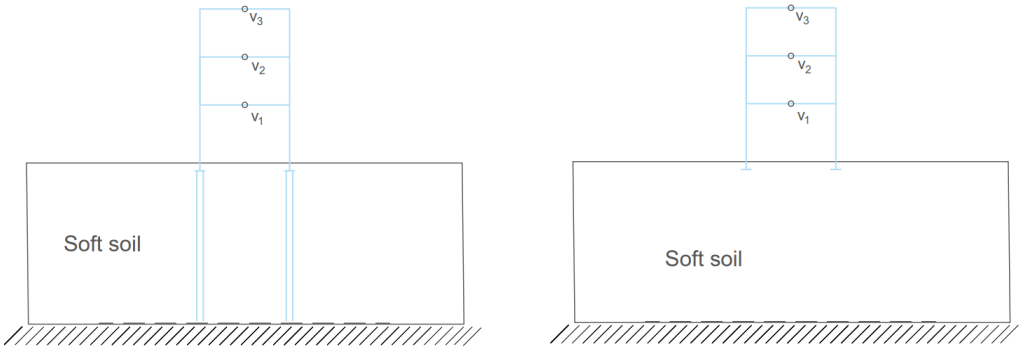

(a) *Case of study with piles groups foundations* (b) *Case of study with slab foundations*

Figure 1.2: *Cases of study taken into account; piles group foundations (a) and slab foundations (b)*

Both the cases of study are characterized by the presence of a soft soil, with shear wave velocity $V_s = 60m/s$, density $\rho = 1750kg/m^3$, Young's Modulus $E_s = 18270000Pa$ and Poisson's ratio $\nu = 0.45$.
The soil, in both cases, is supposed to be composed by one layer of soft soil lying on an horizontal stratum of bedrock.
In the piles groups foundations, where each group is composed by four vertical piles made of concrete with squared cross section, the assumption of end-bearing piles has been made.
In the case of slab foundation, the slabs are made of concrete and they have a squared shape.

Chapter 2

Description of traffic-induced vibrations

Vibrations in a building environment can have different causes, including earthquakes, explosions, and high-speed traffic.
The number of buildings located near railways and highways is on the rise. Therefore, it's crucial to assess how these vibrations affect the structural behavior of buildings. Such vibrations can lead to structural damage, discomfort, malfunctions of sensitive equipment, and even sleep-related health issues for the stakeholders [17].
The transmission of traffic-induced vibrations can be divided into three parts: source, medium, and receiver.
Having precise knowledge about each of these components leads to a more accurate estimation of results. This, in turn, allows for a more precise and efficient approach to mitigating the vibrations that affect the receiver.

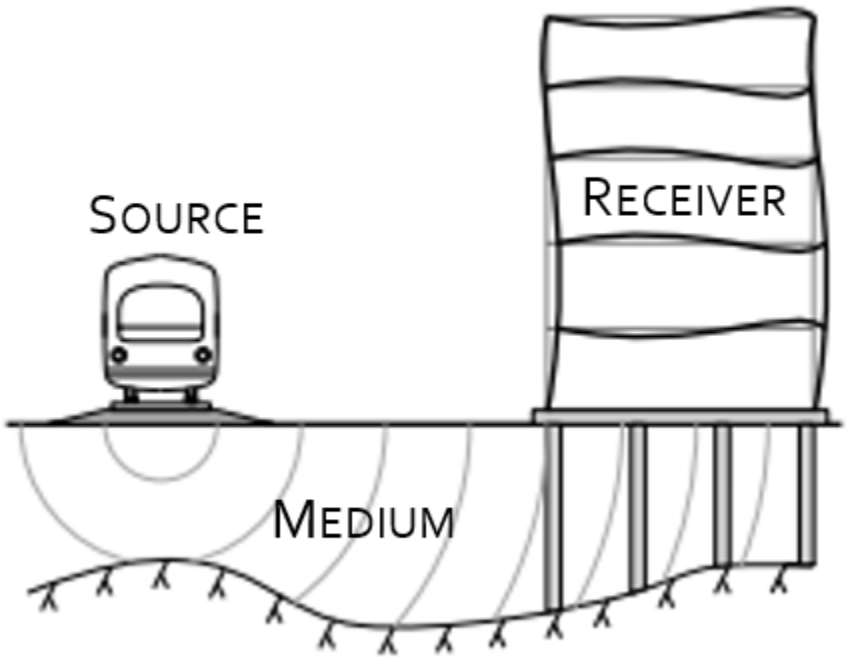

Figure 2.1: *Transmission of vibrations*

The source of vibrations is the infrastructure on which vehicles travel, such as railways or highways.
These vibrations can have different origins. Typically, when a vehicle moves over a road, it causes a time-varying deflection, creating dynamic excitation.
Other factors also contribute to soil vibrations, like irregularities in the asphalt layer of roads or the roughness of railway tracks. Normally, a vehicle that passes on a part of the street, produces a deflection that varies with time, becoming then a dynamic excitation.
Evaluating these irregularities is essential to estimate the frequency and intensity of induced vibrations accurately.
Another influential factor is when a train's speed exceeds the track's critical velocity, resulting in ground vibration amplification beneath the track [11].
According to [6], [3] and [9], the frequency of vibrations induced by highway and high-speed traffic generally stays below 25Hz, although these traffic types may have different frequency peaks.

The medium, in this context, refers to the solid through which the dynamic perturbation from the source travels to the receiver. Depending on the location of the traffic infrastructure, this medium can be a bridge, a tunnel, or the ground. The dynamic properties of this medium, such as material damping and shear wave velocity, play a significant role in how the perturbation propagates through it.
Soil is the most common medium and is typically composed of several layers of different materials resting on a bedrock stratum.
The depth of each layer and the materials they consist of have a substantial impact on how vibrations propagate through the soil.

The receiver, in this context, refers to a structure located near the source, like a building near a railway.
The response of this receiver to induced vibrations can vary due to several factors, including the materials used for construction, foundation type, mass distribution, and isolation measures.
These factors collectively affect the structure's eigenfrequencies, which determine the frequency at which the floors experience peak velocity and acceleration due to resonance.
The maximum allowable vibration level can be determined based on various criteria. For residential buildings, it might be set according to human perception thresholds, while for sensitive equipment, it could be based on their sensitivity to vibrations.

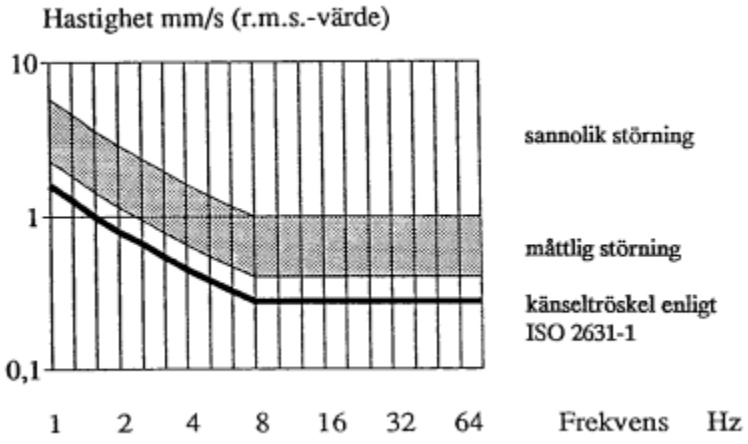

Figure 2.2: *Threshold associated to human perception for vibration level in the receiver, figure source: [18])*

Figure 2.2 shows the threshold stated by the Swedish Standard Institute for human perception of the vibrations, taking into account that human perception is less sensitive to frequencies below 8 Hz.

2.1 Types of waves

The main type of waves that can travel into the soil, described as an elastic half-space, can be divided into body waves and surface waves.
The body waves can travel both on the surface of the ground and in its interior part. Those waves can be divided into shear waves (figure 2.3 (b)), characterized by the motion of particles is transversal to the direction of propagation of the wave, and longitudinal waves (figure 2.3 (a)), that makes the particles move in the same direction of the propagation of the wave.
The velocity of propagation of the wave depends on the soil properties, and can be calculated as follow:

$$V_s = \sqrt{\frac{E}{2 \cdot (1 + \nu) \cdot \rho}} \tag{2.1}$$

and

$$V_p = V_s \cdot \sqrt{\frac{2 \cdot (1 - \nu)}{1 - 2 \cdot \nu}} \tag{2.2}$$

where ρ is the density of the soil, E is the Young's modulus of the soil, ν the Poisson's ratio of the soil and V_s and V_p are respectively the shear wave velocity and the pressure wave velocity of the soil.

Another way to compute the velocity of a shear wave is to use the frequency of the wave and its wavelength. Those parameters are related to the velocity by the following equation:

$$V_s = f \cdot \lambda \tag{2.3}$$

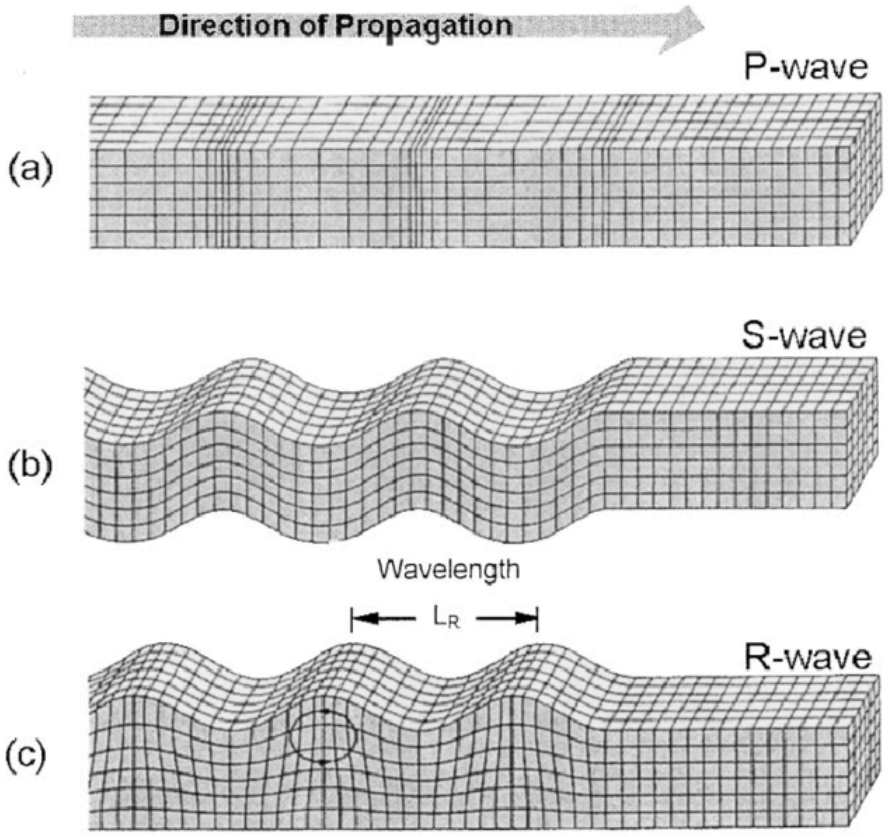

Figure 2.3: *Type of waves in the soil; (a) pressure wave; (b) shear wave; (c) Rayleigh wave. Figure source: [2])*

The surface waves, on the other side, can travel just on the ground surface, in a layer that has a thickness equal to its wavelength.
The most important type of surface wave is the Rayleigh wave (Figure 2.3 (c)). This type of waves presents a motion of the particle in both the vertical and longitudinal direction.
The velocity of propagation is slightly lower than the one of the shear waves, and it can be estimated as:

$$V_r \approx 0.95 \cdot V_s \tag{2.4}$$

This type of wave becomes relevant for great distances from the source, because it carries the biggest amount of energy (70%). On the other side, for low frequencies, that are the ones of interest in engineering practice, the majority of the energy is carried by pressure waves [2].
The surface waves do not propagate in the body of the ground, therefore they do not experience radiation damping, but just material damping. The body waves, instead, are affected by both these damping mechanisms, as long as they travel in all directions in the soil.

2.2 Waves propagation

When a perturbation is introduced at a point within the soil, it initiates the propagation of a wave that spreads throughout the soil.
In cases where there are no body forces acting, the equation governing the motion of a linear elastic medium follows Navier's equation:

$$(\lambda^e + G) \cdot \frac{\partial e}{\partial i} + G \cdot \nabla^2 \cdot u_i = \rho \cdot \frac{\partial^2 u_i}{\partial t^2} \tag{2.5}$$

where i is representing the spatial coordinates x, y, z; e is the volumetric strain, u_i is the displacement associated to the i-th spatial coordinate, ρ is the density, G is the shear modulus of the soil and λ^e is the Lame' operator, defined as:

$$\lambda^e = \frac{2 \cdot G \cdot \nu}{1 - 2 \cdot \nu} \tag{2.6}$$

where ν identifies the Poisson's ratio of the soil.
The amplitude of the vibrations tends to decay the further we observe it from the source point. This is because the further we go from the source, the larger the domain of soil in which the energy of the wave spreads.
In addition to that, another reason why the amplitude decreases, is the fact that the soil is characterized by the presence of damping. More specifically, it can be divided into material damping (experienced by all the types of waves) and radiation damping (experienced just by the body waves).

2.3 Soil damping

When a wave propagates into the soil, it can experience two different types of damping:

- material damping, which is a property of the soil and corresponds to the energy dissipation capacity of the soil under cyclic stress;
- radiation damping, which corresponds to the attenuation of the wave amplitude due to the spread of the area of propagation of the wave.

The total damping that acts on the wave will be defined as:

$$C \approx C_{radiation} + C_{material}$$

2.3.1 Radiation damping

The distribution of a constant quantity of energy over an area that continuously increases leads to an effect of attenuation of the amplitude of the wave.
This mechanism is called radiation damping, and it affects just the body waves.
The attenuation of the vibrations obtained by the radiation damping is a function of the distance between the observation point and the source, and of the type of wave that is taken into consideration.

According to [2], the effect of radiation damping can be expressed by the following equation:

$$w_2 = w_1 \cdot (\frac{r_1}{r_2})^2 \tag{2.7}$$

where w_2 and w_1 are the amplitude of the wave at a distance r_2 and r_1 from the source, while n is an attenuation coefficient that depends on source location, source type and type of wave.
When a foundation is present, the effect of radiation damping is increased, because the wave will be transmitted from the soil to the foundation and then sent back to the soil. This passage of the vibration in the foundation brings to an appreciable loss of energy. That loss of energy is reflected in a higher attenuation of the amplitude of the vibration.

2.3.2 Material damping

This type of damping affects all types of waves when they pass into the soil.
It can be described as the loss of energy given by hysteresis cycles in the soil when a wave passes through it.
When material damping is present, the shear modulus of the material is modified according to the following equation [1]:

$$G^* = G \cdot (1 + 2i\xi_s) \tag{2.8}$$

where ξ_s is the damping ratio of the soil associated to shear waves. The value of the material damping is evaluated according to a frequency-dependent relation. This means that the value of the damping purchased by the hysteresis of the material changes when the frequency of the wave changes.

$$C_{material} = (\frac{2 \cdot K}{\omega}) \cdot \xi_s \tag{2.9}$$

where K is the dynamic stiffness of the soil, ω is the circular frequency of interest and ξ_s is the damping ratio of the soil associated to shear waves.

2.4 Decoupling of displacement field in soil domain

After defining a general case, that is shown in Figure 2.4, where Ω_b is the building domain, Ω_s the soil domain, which is considered as stochastic, Ω_{PML} the boundary element domain, that is considered as deterministic (because the modifications on the incident waves given by uncertainties do not affect the dynamic stiffness of the structure, thanks to the distance between Ω_b and Ω_{PML}) and Σ_{rp} the boundary between Ω_s and Ω_{PML} , the dynamic problem is studied, according to [15] and (REFERENZA), by decoupling the whole domain in two different parts: $\Omega_b \bigcup \Omega_s$ and Ω_{PML} .

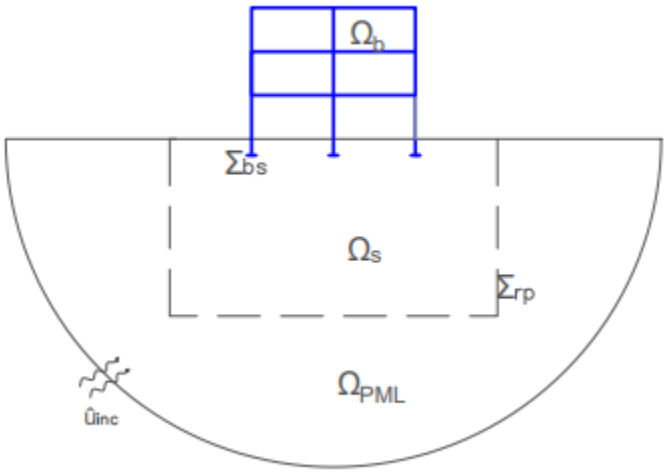

Figure 2.4: *Schematization of model of soil and building*

The whole problem is treated by decomposing the displacement field into three components, as shown in Figure 2.5, in order to compute the traction in the soil domain:

$$\widehat{u}_s = \widehat{u}_{inc} + \widehat{u}_{d0} + \widehat{u}_{sc} \tag{2.10}$$

where:
- $\widehat{u}_{inc}$ is the harmonic free field displacement field generated by an excitation that comes from outside the model;
- $\widehat{u}_{d0}$ is the radiated wave field in the exterior soil domain considering Ω_s as excavated;

it has to satisfy the condition $\widehat{u}_{d0} = -\widehat{u}_{inc}$ on the surface Σ_{rp} ;
- $\widehat{u}_{sc}$ is the scattered displacement field generated in Ω_s as a consequence of the soil-structure interaction and of the soil response.
The first step is the slitting of $\widehat{u}_s$ in two components, that are $\widehat{u}_0$ and $\widehat{u}_{sc}$. $\widehat{u}_0$ is related to the incident waves and it has to be null over Σ_{rp} .

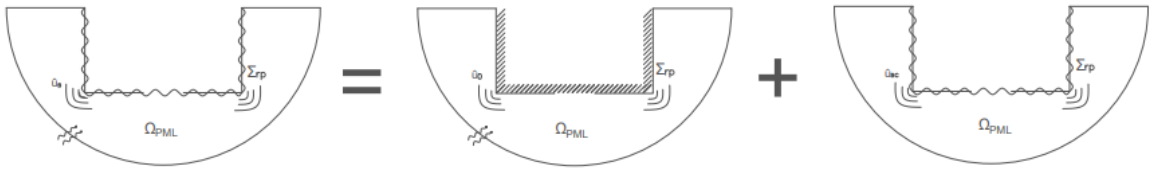

Figure 2.5: *Decomposition of the displacement field*

Due to the complexity of the boundary conditions, it is not computed directly, but it has to be splitted in other two terms:

$$\widehat{u}_0 = \widehat{u}_{inc} + \widehat{u}_{do} \tag{2.11}$$

$\widehat{u}_{inc}$ is defined assuming that the coupling between the source and the receiver can be disregarded.

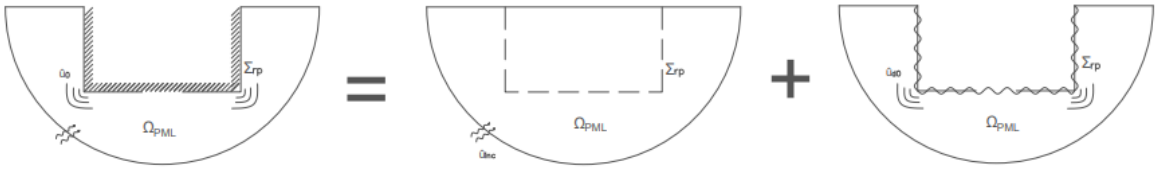

Figure 2.6: *Decoupling between source and receiver*

The equivalent traction of the surface Σ_{rp} evaluated for a load that comes from outside the model is computed by taking in count just $\widehat{u}_{inc}$ and $\widehat{u}_{d0}$, because $\widehat{u}_{sc}$ is given

by the response of the domain of interest.
Infact, the scattering is something that born from the uncertainty of the response, given by the uncertainty of the soil properties.
Than, depending on which type of foundation is assigned to the type of soil (that can be a pile foundation or a slab foundation) the model of the soil will be modified, in order to be able to compute the impedance of the foundations.

Chapter 3

Theoretical background

In this chapter of the Master's thesis, an overview about the theoretical concepts that are involved in the analysis is presented.

3.1 Finite element method

The Finite Element Method (FEM) is a numerical approach used to solve, approximately, whichever type of problem that is governed by a differential equation, like, for example, the deflection of a beam.
While, for simple cases, those differential equations can be solved analytically, in the case of large and complex computational domains, depending also on the type of problem object of study, an approximate solution has to be found.
The Finite Element Method represents a consistent numerical way to solve this kind of problem.
The main principle of this method is the division of the computational domain into, as the name says, elements with finite dimensions.
Each one of these elements, which is representative of the part of the domain to which is assigned, owns its properties, such as, for example, in the case of dynamic problems, a mass matrix and a stiffness matrix, and the final solution is computed on each one of those elements.
From this consideration, it is clear that the finer the size of the elements, the more precise will be the solution, even if, below a certain size of the elements, that depends on the geometry, the loads, the investigated problem and many other factors, the solution

should converge.
The matrices that describe the properties of each element have a size that depends on the number of degrees of freedom considered but also on the discretization of the displacement field chosen.
Those matrices, to find the final solution to the problem, are assembled together, creating a final matrix whose size will take into count of all degrees of freedom present in the model (for example, if the model has n nodes and all the six degrees of freedom are taken in count, the final matrix will have a dimension of $6n*6n$).
The terms relative to a node that belongs to two adjacent elements are summed, because they are related to the same degrees of freedom.
The modeling using FEM allows one to choose both the shape of the elements and the displacement field discretization.
The shape of the element has to be chosen taking into count the shape of the computational domain, choosing the shape of elements that better fits with the geometry of the model. It can be squared or triangular for plane elements, tetrahedral or cubic for solid elements, depending if the computational domain is a 2D model or a 3D model.
The displacement field discretization describes the grade of the polynomial function that will be used for the interpolation or, in other words, how many nodes are present in each element: for example, in a 1D element, a linear discretization creates an element with a node at the beginning and a node at the end of the element, while a quadratic discretization provides an element with a node at the beginning of the element, one at the midpoint and one at the end.
The shape and the discretization of the element are shown in Figure 3.1 for the case of solid elements.

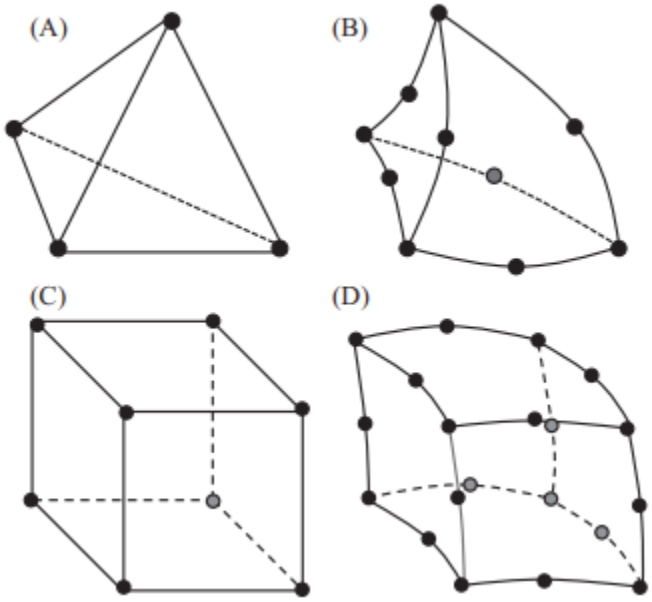

Figure 3.1: *Shape and discretization of finite elements: linear discretization of tetrahedral (A) and cubic (C) element, quadratic discretization of tetrahedral (B) and cubic (D) element; figure source: [4]*

After assembling the big matrices that describe the whole domain discretized with finite elements, the software uses this matrix to solve the model numerically, solving the equation that describes the problem object of the study.
For example, if a static system has to be solved in a FEM model, the equation that describes the problem will be:

$$\mathbf{Ku=f} \tag{3.1}$$

where **K** is the assembled stiffness matrix of the whole system, **u** is the displacement vector that contains the values of all the nodal degrees of freedom, and **f** is the vector of the external forces, that has non-zero elements just in the position that corresponds to the nodes excited by the external forces [16].
As is easily guessable, the more degrees of freedom are present in the model, the greater will be the computational time, so it's worth it, during the modeling process, to think carefully about the size of the element and their discretization, to have the best compromise between the computational time needed and the precision of the solution.

3.2 Structural dynamics

To describe in a simple way the problem of the structural dynamic, is worth it to consider a single degree of freedom system, which schematization is shown in Figure 3.2.

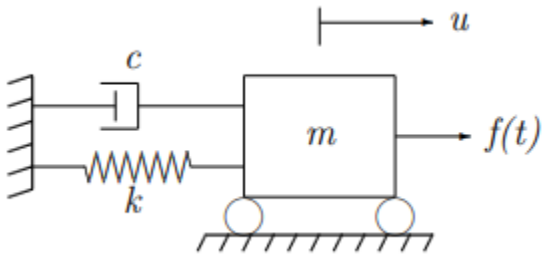

Figure 3.2: *Schematization of a single degree of freedom system excited by a time-dependent force f(t)*

A single degree of freedom system is characterized by a mass m, a stiffness k, which is usually schematized as a spring, and a damping coefficient c.
Those three properties of the system, when multiplied by the acceleration ($\ddot{u}$), the displacement (u), and the velocity ($\dot{u}$) respectively, provide a set of forces.
Using Newton's second law of motion, the equation of motion can be written as follow:

$$m\ddot{u} + c\dot{u} + ku = f(t) \tag{3.2}$$

where $f(t)$ is a time-dependent force applied to the system.
In the case of multi-degree of freedom, as normally structural problems are, the previous equation can be rewritten in matrix form:

$$\mathbf{M\ddot{u}} + \mathbf{C\dot{u}} + \mathbf{Ku} = \mathbf{f}(t) \tag{3.3}$$

3.2.1 Eigenvalue problem

Let's consider an undamped multi-degree of freedom system ($\mathbf{C} = \mathbf{0}$); its equation of motion can be written as

$$\mathbf{M\ddot{u}} + \mathbf{Ku} = \mathbf{0} \tag{3.4}$$

After imposing the boundary conditions, that will determine the values of the constant terms composing the solution, a harmonic solution can be considered as a root of the equation of motion:

$$\mathbf{u}(t) = A\mathrm{e}^{\mathrm{i}\omega t} \cdot \mathbf{\Phi} \tag{3.5}$$

where A is the amplitude of the vibration, $\mathrm{i} = \sqrt{-1}$, ω is the circular frequency and $\mathbf{\Phi}$ is a vector.
After computing the derivative of the harmonic solution and substituting it in the equation of motion, the obtained result is

$$(\mathbf{K} - \omega^2\mathbf{M})\mathbf{\Phi} = \mathbf{0} \tag{3.6}$$

This describes an eigenvalue problem, in which a non-trivia solution can be found by imposing

$$det(\mathbf{K} - \omega^2\mathbf{M}) = 0 \tag{3.7}$$

where a set of $\omega_{n,i}$ will be the solution.
If the MDoF system has k degrees of freedom, the number if $\omega_{n,i}$ that solve the eigenvalue problem will be exactly equal to k.
Once found a specific eigenfrequency $\omega_{n,j}$, introducing this value in the equation 3.1, is possible to evaluate the correspondent eigenmode, that is represented by the vector $\mathbf{\Phi}_j$.

3.2.2 Resonance

Let's consider an undamped single degree of freedom system ($c = 0$), excited by a harmonic force $p_0 \cdot sin(\omega t)$, where p_0 is the amplitude of the force and ω its circular

frequency.
The equation of motion for this type of system will be:

$$m\ddot{u} + ku = p_0 \cdot sin(\omega t) \tag{3.8}$$

As known, the solution of this differential equation will be the sum of the solution of the homogeneous associated differential equation and the particular solution.
The solution of the homogeneous-associated differential equation will be:

$$u_0(t) = Acos(\omega_n t) + Bsin(\omega_n t) \tag{3.9}$$

where A and B are constants that can be determined by imposing boundary conditions on displacement and velocity and ω_n is the natural circular frequency of the system.
The term $u_0(t)$ represents the transient response of the system, which is the response of the system at the moment in which the external load is applied, and it will vanish with time.
The particular solution, instead, is found to be:

$$u_p(t) = \frac{p_o}{k} \cdot \frac{1}{1 - (\omega/\omega_n)^2} \cdot sin(\omega t) \tag{3.10}$$

The term $u_p(t)$ represents the steady-state response of the system, which is the response of the system once the transient response has vanished.
As is clearly noticeable, when $\omega \to \omega_n \Rightarrow u_p(t) \to \infty$.

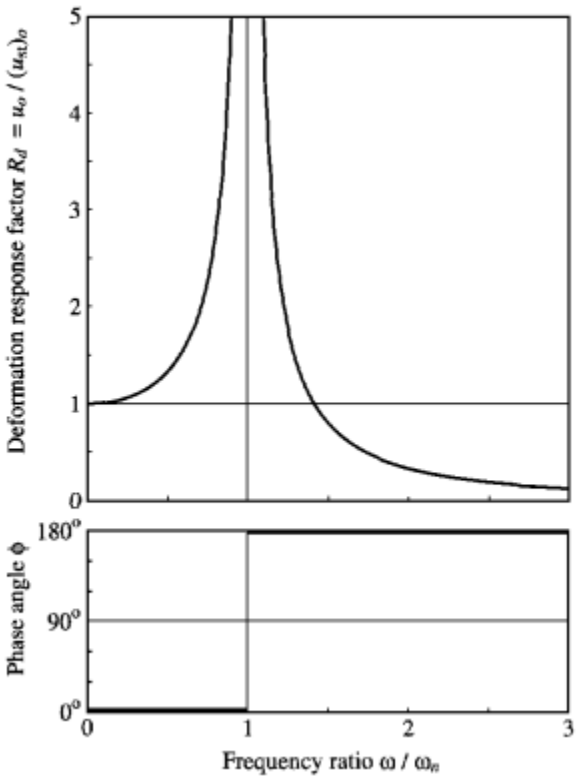

Figure 3.3: *Deformation response factor and phase angle for undamped SDoF,* $R_d = \frac{1}{1-(\omega/\omega_n)^2}$*, figure [5]*

This brings the total displacement, in the absence of damping, to be infinite.
It means that at every cycle to which the system is subjected, the displacement from the initial position tends to grow. This phenomenon is called resonance.
As long as damping is present in all the structural systems, the response will never tend to infinite, but it will reach a maximum threshold, as shown in Figure 3.4.

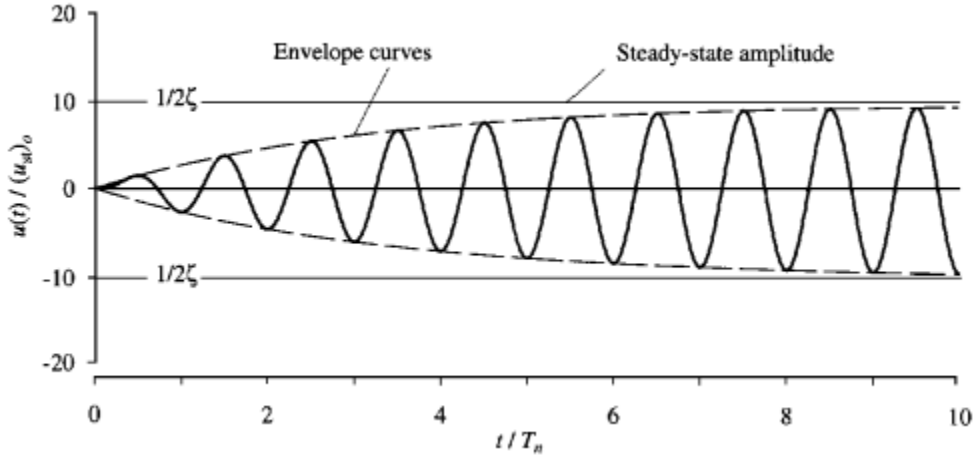

Figure 3.4: *Response of a damped system when the sinusoindal force has the same frequency of the natural frequency of the system, figure source:chopra*

When the frequency domain is taken into consideration, the resonance frequencies of a damped system are the ones to which correspond peaks in the function that describe for example the displacement of the mass of the system. Normally, the sharper the function around the resonance frequency, the lower the damping associated to that frequency and to that mode of vibration.

3.3 Non-reflecting boundaries - PML

Soil modeling often involves treating it as a half-space. However, as the computational domain grows larger, it leads to increased computational time. To address this, a mathematical tool called the Perfectly Matched Layer (PML) can be employed.
PML extends the spatial coordinates into a domain where wave attenuation is higher. This higer level of attenuation of the waves is obtained through a stretching of the spatial coordinates. This stretching minimizes wave reflections at the fixed boundary, enabling the truncation of the computational domain.

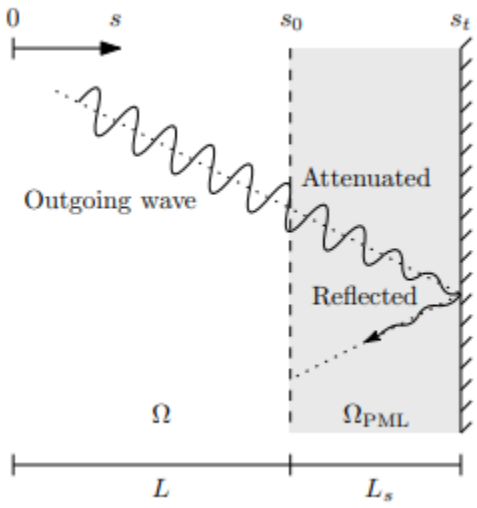

Figure 3.5: *Schematization of the effect of PML on the wave amplitude; figure source: [10]*

With this purpose, the PML has to be perfectly matched with the computational domain at its outer boundary. This is achieved by applying a complex coordinate stretching, which is obtained by using the following equation to transform the coordinates:

$$s \Rightarrow \tilde{s} = s_0 + \int_{s_0}^{s_1} \widehat{\psi}_s(s)\, ds \tag{3.11}$$

where s is the coordinate in the computational domain, $\tilde{s}$ is the coordinate in the PML domain, s_0 is the coordinate at the boundary of the computational domain and $\psi_s(s)$ is the stretching function.
As is clearly noticeable, at the boundary between the computational domain Ω and the PML domain Ω_{PML}, this formulation provides that the points have the same coordinate, achieving the demand of continuity between domains.
As long as in the PML domain the coordinate stretching is considered, the derivatives of the functions that regard stress and strain assume this formulation:

$$\frac{\partial}{\partial \tilde{s}} = \frac{1}{\widehat{\psi}_s(s)} \cdot \frac{\partial}{\partial s} \tag{3.12}$$

This means that, while the relationship between stress and displacement, for what

regards the computational domain, in the frequency domain, can be expressed as

$$\widehat{\sigma}_{ij,j} = -\omega^2 \cdot \rho \cdot \widehat{u}_i \tag{3.13}$$

in the case of the PML domain Ω_{PML} it becomes

$$\frac{1}{\widehat{\psi}_j} \cdot \widehat{\sigma}_{ij,j} = -\omega^2 \cdot \rho \cdot \widehat{u}_i \tag{3.14}$$

or, if written with vector notation, making explicit all the terms:

$$\begin{bmatrix} \frac{1}{\widehat{\psi}_x} \cdot \frac{\partial}{\partial x} & 0 & 0 & \frac{1}{\widehat{\psi}_y} \cdot \frac{\partial}{\partial y} & 0 & \frac{1}{\widehat{\psi}_z} \cdot \frac{\partial}{\partial z} \\ 0 & \frac{1}{\widehat{\psi}_y} \cdot \frac{\partial}{\partial y} & 0 & \frac{1}{\widehat{\psi}_x} \cdot \frac{\partial}{\partial x} & \frac{1}{\widehat{\psi}_z} \cdot \frac{\partial}{\partial z} & 0 \\ 0 & 0 & \frac{1}{\widehat{\psi}_z} \cdot \frac{\partial}{\partial z} & 0 & \frac{1}{\widehat{\psi}_y} \cdot \frac{\partial}{\partial y} & \frac{1}{\widehat{\psi}_x} \cdot \frac{\partial}{\partial x} \end{bmatrix} \cdot \begin{bmatrix} \widehat{\sigma}_{xx} \\ \widehat{\sigma}_{yy} \\ \widehat{\sigma}_{zz} \\ \widehat{\sigma}_{xy} \\ \widehat{\sigma}_{yz} \\ \widehat{\sigma}_{zx} \end{bmatrix} + \omega^2 \cdot \rho \begin{bmatrix} \widehat{u}_x \\ \widehat{u}_y \\ \widehat{u}_z \end{bmatrix} = \mathbf{0} \tag{3.15}$$

With regard to the stretching function, the solutions that can be found in the literature are a lot.
The choice has been to take into count a stretch function which has a real part that is independent of the frequency content, and an imaginary part that varies when the frequency changes.
The stretch function can be written as follow:

$$\widehat{\psi}_s(s) = 1 + f_s^e(s) - i \cdot \frac{f_s^p(s)}{a_0}; \tag{3.16}$$

$$a_0 = \frac{\omega \cdot L_s}{V_s} \tag{3.17}$$

where $f_s^e(s)$ is the real scaling parameter of the stretch function, $f_s^p(s)$ the imaginary

scaling parameter of the stretch function, $i = \sqrt{-1}$, ω is the circular frequency, L_s the thickness of the PML domain and V_s the shear wave velocity of the soil.
The choice of taking a stretch function in which the real scaling parameter is not frequency dependent allows to have a simple correlation between the stretch function and the term $i\omega$. This allows applying easily the Inverse Fourier Transform, enabling the switch to time domain analysis in case of need.
The stretch function operates with Cartesian coordinates. This means that the mesh of the PML has to be composed of squared elements, otherwise, the stretching of the coordinates will be done in a wrong way, bringing to unreliable results.
As the frequency of the wave rise, the stretching on coordinates has to be greater. This is translated into a greater stretching parameter of the real part and into a smaller value of the size of the elements. Infact, to properly represent a wave, there have to be at least 12 nodes per wavelength.

3.4 Impedance functions

When a foundation is present on the soil, at the contact surface, being the foundation loaded by a force $F(t)$, there will be a reaction of the soil $P(t)$. For the d'Alambert principle, will rise an inertial force $m\ddot{u}$, where u_z is the displacement of the foundation and m is the mass of the foundation ($\ddot{u}_z$ is the acceleration), as shown in the figure 3.6.
So the dynamic equilibrium of the foundation will be described by the following equation:

$$P_z(t) + m\ddot{u}_z(t) = F_z(t) \tag{3.18}$$

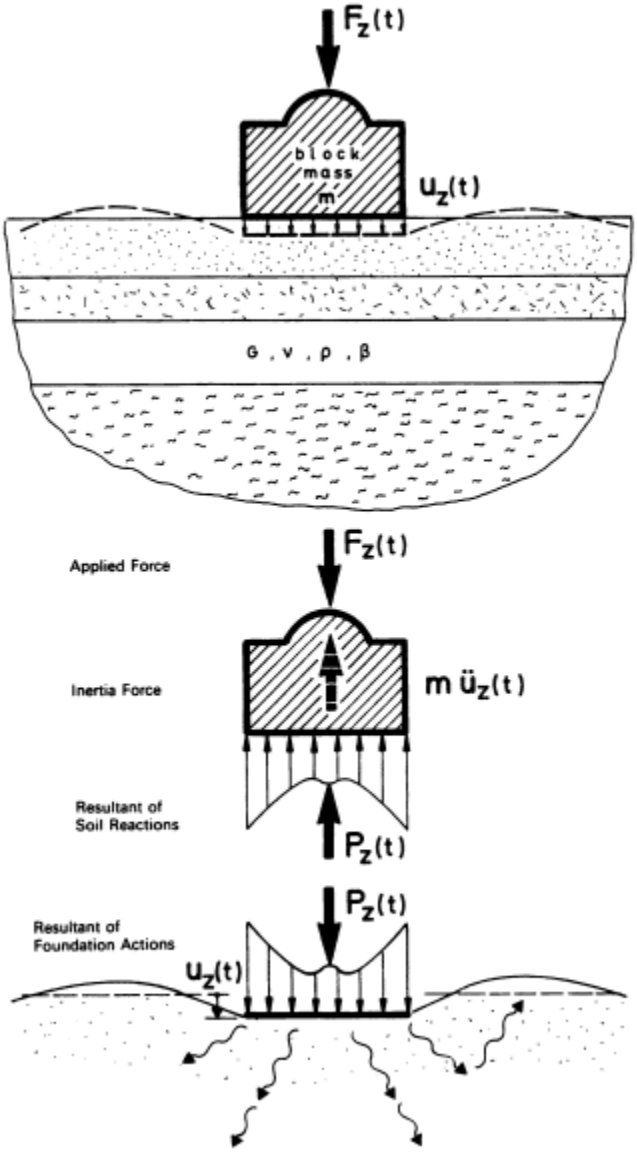

Figure 3.6: *Vertical equilibrium of a foundation block; figure source: [8]*

Assuming that the contact force between soil and foundation can be written as:

$$P_z(t) = \chi_z \cdot u_z(t) \tag{3.19}$$

and substituting equation 3.19 into equation 3.18, is clear that the term χ_z can be expressed as follow:

$$\chi_z = \frac{(F_z(t) - m\ddot{u}_z)}{u_z} \tag{3.20}$$

The term χ_z is called Impedance, it is frequency dependent and describes the interaction between the foundation and the soil.
It is defined as the contact force between the soil and the foundation divided by the displacement of the foundation.
The value of the impedance is a complex number, in fact, it can be expressed as follow:

$$\chi_z = K_z + i\omega C_z \tag{3.21}$$

The real part is the dynamic stiffness. It describes the stiffness and inertia of the soil when the foundation is present (its frequency dependence is given by the fact that the inertia of the foundation, which is a dynamic property, is involved). The imaginary part, instead, when divided by the circular frequency, represents the sum of material damping and radiation damping, properties described in section 2.3.
As just stated for the vertical case, the direct terms of the impedance can be described in the exact same way for all the other degrees of freedom. This can be achieved by imposing a displacement along a certain direction (or a rotation around a certain axis) and looking at the reaction force in that same direction (or to the reaction moment around the same axis).
Also coupled terms of the impedance can be taken in count.

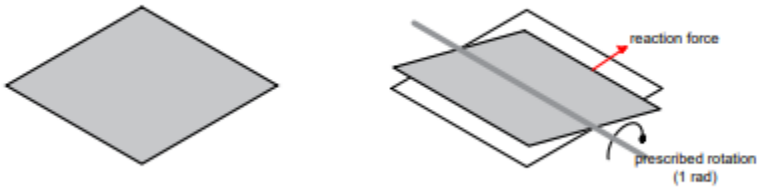

Figure 3.7: *Schematization of the computational process of coupled terms of impedance on a slab foundation*

As shown in Figure 3.7, in order to compute coupling terms of the impedance matrix, it is necessary to apply a rotation around an axis and look at the reaction force along the perpendicular in-plane axis (or apply a displacement along an axis and look at the reaction moment around the perpendicular in-plane axis).
After computing all the direct and coupling terms of the impedance, the impedance matrix can be built in this way:

$$[\chi](\omega) = \begin{bmatrix} \chi_{xx} & \chi_{\theta_x y} & 0 & 0 & 0 & 0 \\ \chi_{\theta_y x} & \chi_{yy} & 0 & 0 & 0 & 0 \\ 0 & 0 & \chi_{\theta_x \theta_x} & \chi_{x\theta_y} & 0 & 0 \\ 0 & 0 & \chi_{y\theta_x} & \chi_{\theta_y \theta_y} & 0 & 0 \\ 0 & 0 & 0 & 0 & \chi_{zz} & 0 \\ 0 & 0 & 0 & 0 & 0 & \chi_{\theta_z \theta_z} \end{bmatrix} \tag{3.22}$$

where the terms on the diagonal are the direct terms of the impedance function, while the non-diagonal terms are the coupling terms.

Chapter 4

Methodology

The primary goal of this work is to demonstrate the reliability of a computational method. To achieve this, a comparison must be made between a reference solution and the obtained results. This involves creating not only the FEM-PML models used for computing impedances, foundation displacements, and floor velocities, but also an additional FEM-PML model. The additional model encompasses the soil, foundation, and building and serves as the reference solution. It's important to note that the computational time for this reference model is quite high.
This chapter provides an overview of the types of computations conducted, explains how the MatLAB code for applying the external load simulating traffic functions, and offers a detailed breakdown of how the problem was divided into multiple steps.

4.1 Performed calculations

With the aim to give the reader a better understanding of the work done, a list of the performed calculations is shown in this section.
All the analyses that are listed here have been conducted for both cases of study, which are described in Section 1.2.

- To compute the terms of the impedance matrix for the soil-foundation system, a small model was used. This model included just one foundation group. In this model, a unitary displacement (or rotation) was assigned, while all other possible displacements and rotations were locked.

The impedance's value is determined by the reaction force (or reaction moment) that emerges in the system as a result of the imposed displacement or rotation. A 2D schematization of the model is shown in Figure 4.1.

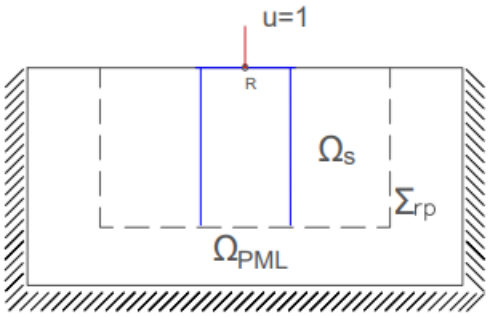

Figure 4.1: *2D schematization of the FEM-PML model for the impedance calculation*

- The foundation displacements were computed using two different methods.
  First, a small model (Figure 4.2(a)) with just one foundation group was utilized. An external load, applied using the MatLAB code described in Section 4.2, was used to calculate the foundation displacement caused by traffic-induced vibrations. Initially, the load was placed 12 meters from the center of the foundation, and later at a distance of 18 meters. This accounts for the real positions of the foundation groups.
  Second, a larger model (Figure 4.2(b)) containing all four foundation groups was employed. Similar to the small model, an external load applied with the MatLAB code described in Section 4.2, has been used to compute the foundation displacement given by the vibration caused by the traffic load.
  In this case, the load was positioned 15 meters away from the center of the model. This allowed for two foundation groups to be 12 meters from the load, and the other two foundation groups to be 18 meters distant from the source of vibrations. The decision to compute the displacements twice for each foundation group was made to enable a comparison of the computed displacement values and to check if the presence of other foundation groups had any impact on the results.

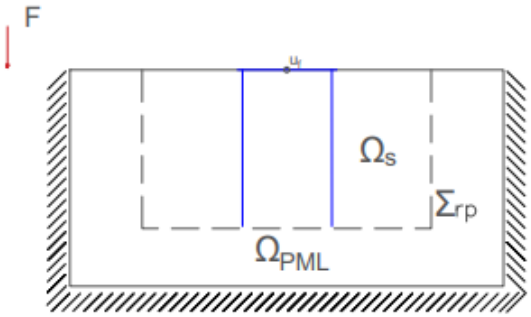

(a) *Foundation displacement on small model (just one foundation group) calculation*

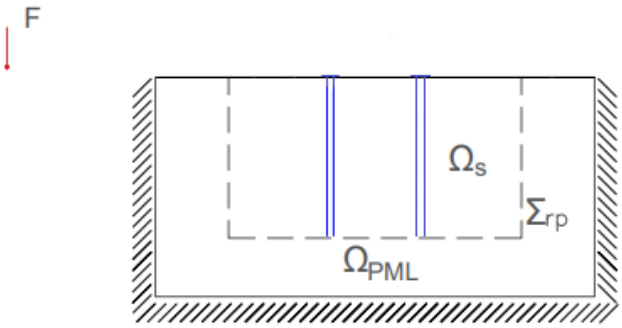

(b) *Foundation displacement on big model (all four foundation groups) calculation*

Figure 4.2: *2D schematization of the FEM-PML models used to perform the calculation of foundation displacement given by an external load*

- Velocities of the floors were computed using an FEM model of the reference building, excluding the soil domain. The 2D schematization of this building is shown in Figure 4.3.

  To account for the soil's influence, impedances were applied as a set of springs and dashpots under the building.

  The building's excitation was based on the previously computed foundation displacements, which were applied as a base motion.

Specifically, for the two front columns, the displacements computed for foundations positioned 12 meters from the point load were used.
For the two columns at the back, the base motion was determined using the displacements computed for foundations 18 meters away from the point load.
To assess the impact of the distance between the front and back foundations on the results, these displacements were modified by introducing a frequency-dependent phase shift. Subsequently, the analysis was repeated.
As a result of the analysis, velocities at the midspan of the floor slabs were recorded and plotted against frequency.

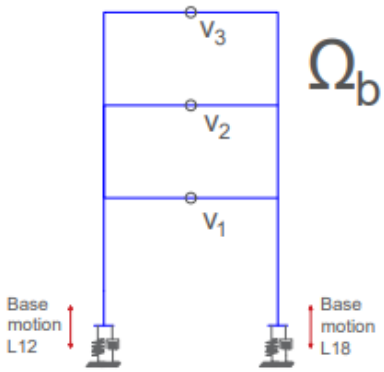

Figure 4.3: *2D schematization of the FEM model of the reference building*

- The reference solution is represented by a FEM-PML model comprehensive of soil, foundations and superstructure, which 2D schematization is shown in figure 4.4.
  The model is loaded by an external load applied at 15 m from its center by using the MatLAB code described in Section 4.2. The velocities of the floors are evaluated and plotted against frequency.
  This represents the usual way in which the problem of ground-borne vibration is treated. Therefore, the results obtained by using the method object of study are compared to the ones that come from this analysis.

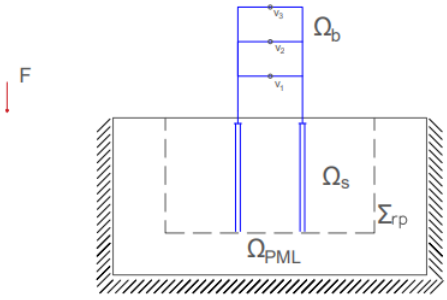

Figure 4.4: *2D schematization of the FEM-PML model of soil, foundation and building excited by an external load, which represents the reference solution*

4.2 External load

In order to assess the effects of the traffic load, it is crucial to include it in the model alongside the soil. However, it is equally important to keep the computational domain as compact as possible to avoid extensive computational time. Therefore, the load must be modeled in a manner that permits its inclusion without enlarging the soil domain.

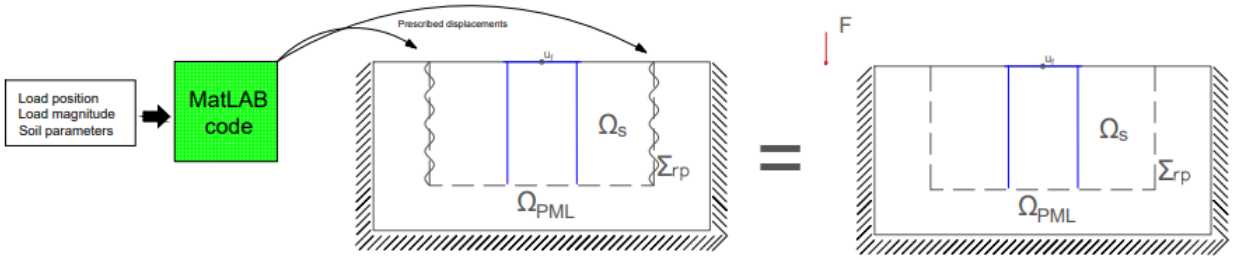

Figure 4.5: *Schematization of the application of the external load*

The MatLAB code that has been used to introduce the traffic load in the model has been thought with this exact purpose: introducing the load at whichever distance from the center of the soil domain without enlarging the soil domain itself.
This is achievable through the translation of the load into the displacements that it is expected to induce at the boundary of the soil domain

The MatLAB code will create a Comsol model, with the desired properties, geometry and, most of all, with the presence of the displacements that simulate the presence of the traffic load.
Before running it, the properties and the geometry of both soil and foundation, the magnitude and the position of the load, the properties of the PML and the size of the mesh needed have to be inserted.
After the introduction of the needed informations, the MatLAB code works in this way:

- The shear wave velocity and the pressure wave velocity are computed starting from Young´s modulus, Poisson ratio and density of the soil that have been defined by the user, considering the material as isotropic; then the model of soil and foundation with the PML layer is generated.

- Nodal coordinates, Gauss coordinates and inwards surface normals of the boundaries between the computational domain and the PML regions of the Comsol model are extracted.

- The displacements and tractions at the boundary faces of the Comsol FEM-PML model given by a point load are computed. The code uses Green's functions of a layered halfspace, which are computed using an external toolbox called ElastoDynamicToolbox.
  This procedure is iterated over each boundary face and it provides the computation of the displacements at the nodes and stresses at the Gauss points.

- The prescribed displacements are assigned to the boundary between the soil domain and the PML. The soil is considered as excavated, in order to compute the traction field of the excavated soil domain (referred to the approach described in 2.4, where the displacement field realtive to the excavated soil is called $\widehat{u}_0$).
  Those traction are added to the ones computed before.

- The traction field is interpolated and stored in a tab per each frequency of interest.

- Having traction field that represent the effect of a point load situated outside the computational domain per each point of the surface between the computational soil domain and the PML, the correspondent displacement field is computed and interpolated.

- The displacement field generated computed using the traction field is added to the Comsol model, as shown in Figure 4.6.

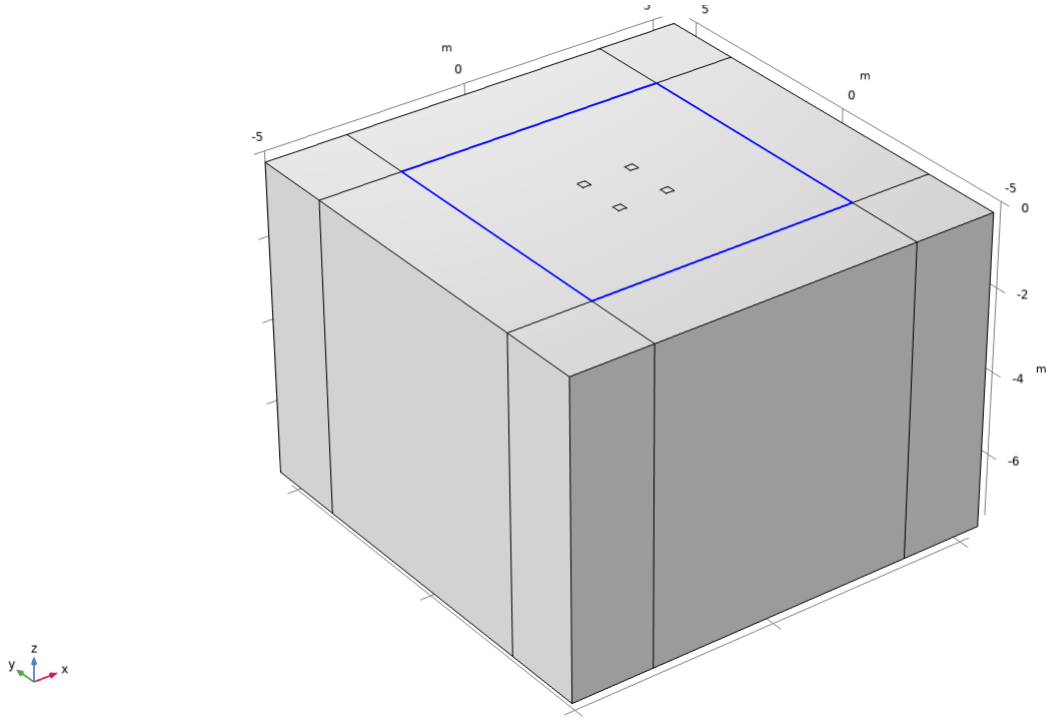

Figure 4.6: *Pile group foundation model with the prescribed displacement field that simulate the external load shown*

4.3 Procedure

The procedure that has been followed to carry on this study is divided between the creation of the model which represents the reference solution and the set of models needed in order to divide the problem in more steps that are less time-demanding.
The model of the reference solution has greater dimension with respect to the models to

which sections 4.3.2 and 4.3.3 refer to, because it contains all the four foundation groups.

4.3.1 Reference solution

The reference solution consists in a FEM-BEM model which contains a large soil domain. This soil domain is comprehensive of all the foundations groups, and the whole building, as shown in figure 4.7.

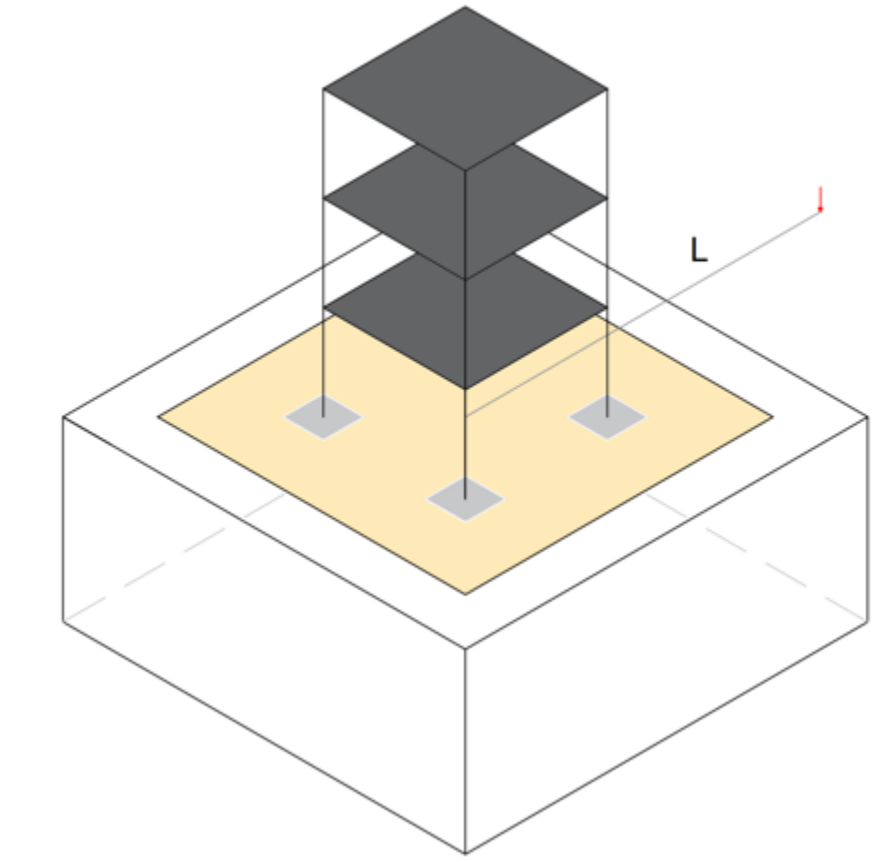

Figure 4.7: *3D Schematization of the FEM-PML model used to compute the reference solution; in yellow the soil computational domain, in white the PML domain*

A unitary load, simulating traffic, is applied at a distance (L=15m) from the center of the soil model. This is accomplished using the MatLAB code described in Section 4.2. The code allows modeling the load as a prescribed displacement at the edge of

the computational domain. This approach permits placing the load outside of the soil domain, eliminating the need for a larger model to apply the load.
Following the computation in the frequency domain, where the input load is applied as prescribed displacements on the boundary between the PML domain and the computational domain, the key results considered are the velocities and accelerations of the building's floors.

4.3.2 Impedances

To account for the soil's impact in a Finite Element Method (FEM) model with only the superstructure, it's possible to evaluate the dynamic properties of the soil-foundation system. These properties can then be introduced as parameters, describing a set of springs and dashpots beneath the building's foundation.
This is achieved by using the impedances computed on a single foundation group.
As discussed in Section 3.4, impedance can be expressed as the ratio between the reaction force of the soil to the foundation's movement and the displacement of the foundation. Equation 4.1 (for translational impedance in the z direction) provides a description of this relationship.

$$\chi_z = \frac{P_z}{u_z} = K_z + i\omega C_z \tag{4.1}$$

According to this, in order to compute the impedances, a unitary displacement (or rotation) has been imposed on the center of the foundation, as shown in figure 4.8. Then, the reaction forces and reaction moments have been taken as results.

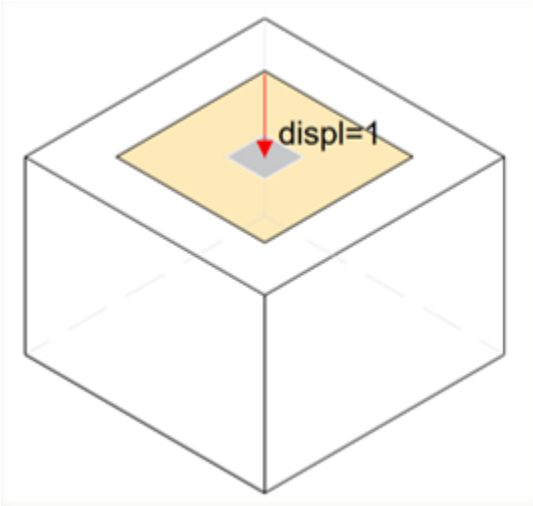

Figure 4.8: *3D Schematization of the FEM-PML model used to compute the impedance, case of slab foundation; in yellow the soil computational domain, in white the PML domain*

The values of the reaction forces and reaction moments already represent the terms of the impedance matrix. In a second moment, with the help of MatLAB, the real part and imaginary part of the impedances have been splitted, in order to evaluate dynamic stiffness and damping.

4.3.3 Computed displacements

To incorporate the impact of the traffic load into the superstructure model, where the soil is represented by a set of springs and dashpots, it's essential to first determine the displacements of the foundation groups.
To achieve this, a small soil model was created, and an external load was applied. Initially, the load was placed at a distance of L = 12 meters from the center of the foundation, and subsequently, it was positioned at a distance of L = 18 meters. The setup for those computations is illustrated in Figure 4.9.

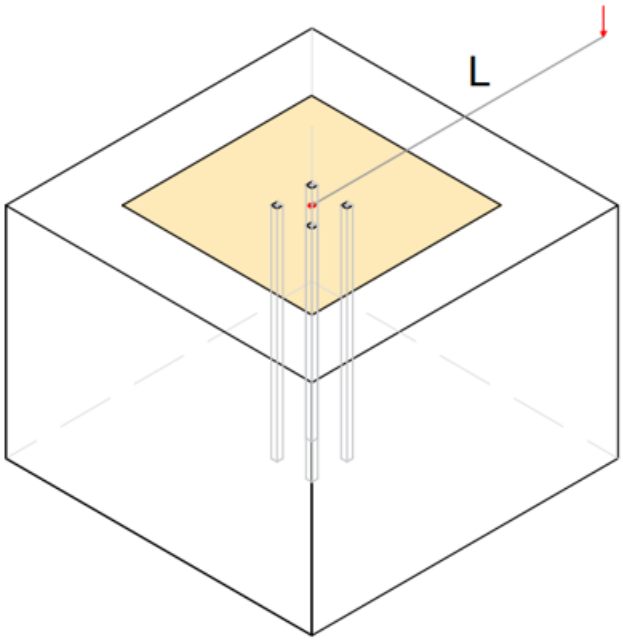

Figure 4.9: *3D Schematization of the FEM-PML model used to compute the displacements of the foundations group, case of pile group foundation; in yellow the soil computational domain, in white the PML domain*

In these models, no forces are present within the computational domain. Instead, the perturbation is introduced through a prescribed displacement applied to the boundary of the computational domain. This displacement mimics the presence of a unitary load positioned at a distance (L) from the center of the model, which is also the center of the foundation group.
For each type of foundation, the model was run twice: once with L=12 meters and once with L=18 meters, considering the varying positions of the foundation groups.
Additionally, the displacements of the foundation groups were computed within the model containing all four foundation groups. In this case, the external force was assumed to be 15 meters away from the center of the model. This approach was taken to investigate whether the presence of other foundation groups influenced the results.

4.3.4 Building on spring and dashpots

To determine the amplitude of velocity and acceleration on the floors of the building, two models were developed—one for each type of foundation. These models featured the building, and at their foundations, they incorporated a set of springs and dashpots, as illustrated in Figure 4.10.

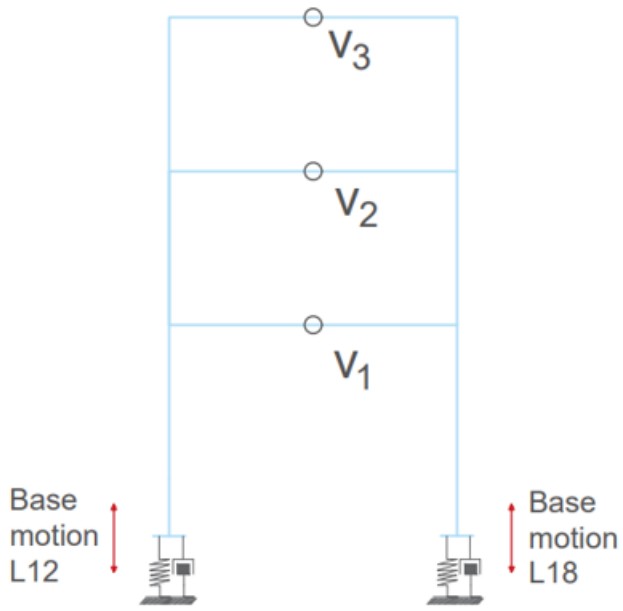

Figure 4.10: *2D schematization of the FEM model used to compute the velocities and the acceleration on the building over spring and dashpots with an applied base motion*

At the bottom of each column, there is a set of springs and dashpots that schematize the impedance of the system soil-foundation, which computational method has been described in section 4.3.2.
This is because, alternatively to FEM-BEM models, simple physical models can be used to describe the force-displacement interaction of the foundation ([19]). Despite what the figure 4.10 shows, not just the vertical impedance, but also the rocking and transversal terms are taken in count.
After, during a second analysis, also the coupling terms are taken in count, in order to evaluate the effect of their presence on the results.
The displacements computed according to what is stated in section 4.3.3, have been

introduced as a base motion at the bottom of the spring-dashpots sets (in the Comsol model, the base motion is the source point for the spring-dashpot command, while the end of the column is the destination).
As the perturbation does not arrive at the same moment in all the foundations, the phase shift present between the moment in which the foundations at L = 12 m and the ones at L = 18 m has been taken into count in a second analysis to evaluate the effect of its presence on the results.
After computing the phase angle per each frequency of interest, the displacements of the foundations at L = 18 m from the load have been computed in three different ways. This has been done to understand which is the most efficient way to model the phase shift for the foundation displacements:

- $$A_{18,new} = A_{18} \cdot cos(\theta) \tag{4.2}$$

  where A_{18} is the amplitude of the evaluated displacement on the foundations when L = 18 m and θ is the phase angle.
  In the following chapters, this way of modeling the phase shift is named "phase shift 1"

- $$A_{18,new} = A_{18} \cdot e^{i\theta} \tag{4.3}$$

  where A_{18} is the amplitude of the evaluated displacement on the foundations when L = 18 m and θ is the phase angle.
  In the following chapters, this way of modeling the phase shift is named "phase shift 2"

- Displacement computed as a complex number and not as a displacement amplitude, obtained directly from the FEM-PML models described in Subsection 4.3.3.
  In the following chapters, this way of modeling the phase shift is named "phase

shift 3”

Then, after a frequency domain analysis, the velocity and the acceleration at the midspan of the three floors are the results of interest.

Chapter 5

Numerical models

Several models have been created in order to analyze this problem:

- one model for the building on fixed constraints, that in a second moment has been modified with the addition of spring and dashpots in the place of the fixed constraints, with the aim to simulate the impedance;
- one model with a single foundation group, to compute the impedances;
- one model with a single foundation group and external load, to compute the displacement of the foundations given by traffic load;
- one model comprehensive of soil, foundations, building and external load, which represents the reference solution.

Having two cases of study (one that takes into count piles foundation and the other that takes into count slab foundation, described in Section 1.2), for each case of study all these models have been created and analyzed.
The software used is Comsol and the models with the soil have been created utilizing the MatLAB code described in Section 4.2. This code allows one to choose the position of the foundations, the parameters of the soil, and also to introduce an external unitary load, utilizing the ElastoDynamicToolbox.

5.1 Building

The building that has been taken into consideration, in order to study this kind of problem, is a really simple three-story building, shown in Figure 5.1. Its parameters have been chosen with the aim to have three different natural frequencies for what regards the vertical ways of motion.

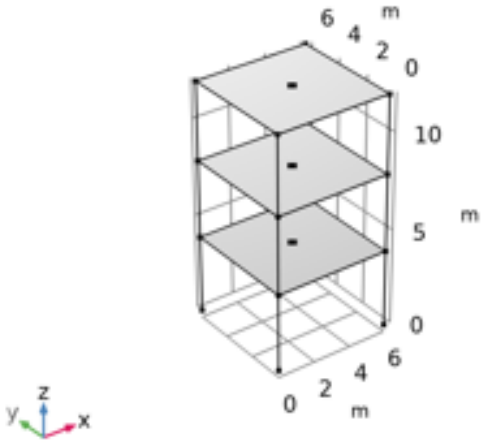

Figure 5.1: *Building model in Comsol*

The span in the x direction is the same of the one in the y direction and it is equal to 6 m. The height of the building has been set as 12 m, introducing a floor slab every 4 m.
Columns and beams are composed of the same material, that is structural steel, which has the following parameters:

- Young's modulus $[Pa] = 2.1 \cdot 10^{11}$
- Poisson ratio $[-] = 0.3$
- Density $[kg/m^3] = 7850$
- Damping ratio $[\%] = 2$

The cross-section of both columns and beams has been chosen to be a Hollow-Box section, as shown in Figure 5.2, even if their dimension are different.

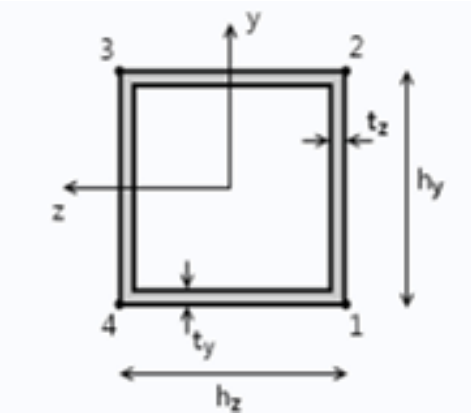

Figure 5.2: *Cross section geometry of beams and columns*

For what regards the columns, the cross-section has the following dimensions:

- $h_y = h_z = 0.4m$,
- $t_y = t_z = 0.04m$;

for what regards the beams, the cross-section has the following dimensions:

- $h_y = h_z = 0.3m$,
- $t_y = t_z = 0.03m$.

The index h_y, h_z, t_y and t_z are referred to Figure 5.2.

In the case of the floor slabs, the material that have been chosen is concrete and it has the following parameters:

- Young's modulus $[Pa] = 3.4 \cdot 10^{10}$
- Poisson ratio $[-] = 0.2$
- Density $[kg/m^3] = 2400$
- Damping ratio $[\%] = 2$

The thickness of the three floor slabs is different: the slab at $z = 4m$ has a thickness equal to $0.2m$, the one at $z = 8m$ has a thickness equal to $0.14m$ and the one at $z = 12m$ has a thickness equal to $0.1m$.
Each floor slab has an added mass of $500kg/m^2$ and at the bottom of each column.

A lumped mass of $5057.5kg$ has been placed, in order to simulate the weight of the foundation slab.
The linear elements, such as beams and columns, have been modeled as Timoshenko beams, in order to take into account also the shear deformation during the analysis.
The elements of the mesh have chosen to have a cubic displacement field, because being linear elements they don't have too many degrees of freedom. Therefore, is worth it to have a higher grade of the polynomial function used to interpolate the displacement field in order to have more precise results.
The floor slabs, instead, have been modeled as shells, and squared elements with a quadratic displacement field.
The connection between the shells and the beams has been imposed on all the shared edges. This has been done in order to guarantee the continuity of displacements at the interface between the floor slabs and the beams that are supposed to bear those slabs.
The size of the element composing the mesh has been chosen to be the same for shells and beams, and its value is equal to $0.25m$.

5.1.1 Eigenfrequencies

The results that have been obtained after running an eigenfrequency analysis of the structure with fixed constraints are shown below. The first three sway modes of vibration and the first three vertical modes of vibration are shown in Figure 5.3 and Figure 5.4, respectively.

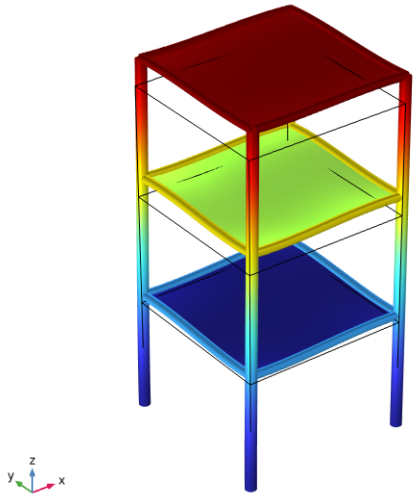

(a) *First sway mode of vibration,* $f = 2.29Hz$

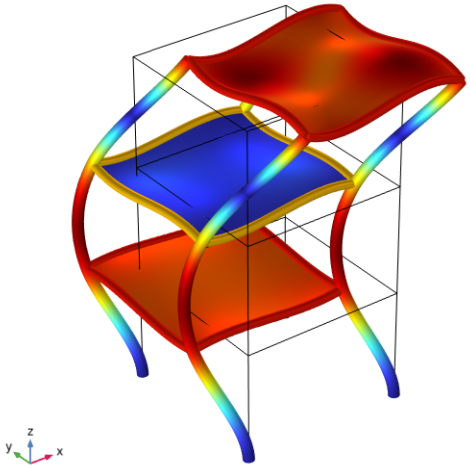

(b) *Second sway mode of vibration,* $f = 7.96Hz$

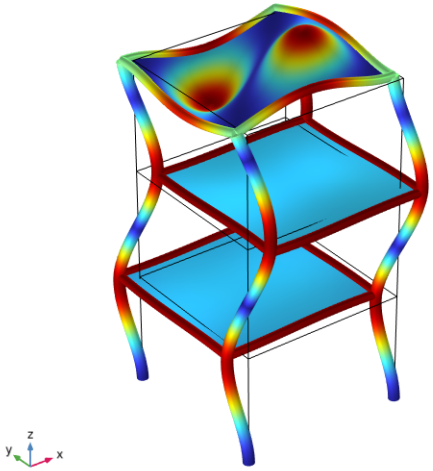

(c) *Third sway mode of vibration,* $f = 16.33Hz$

Figure 5.3: *First three sway modes of vibration of the building*

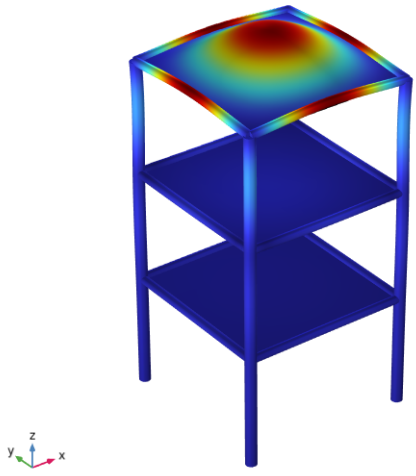

(a) *First vertical mode of vibration,* $f = 7.80Hz$

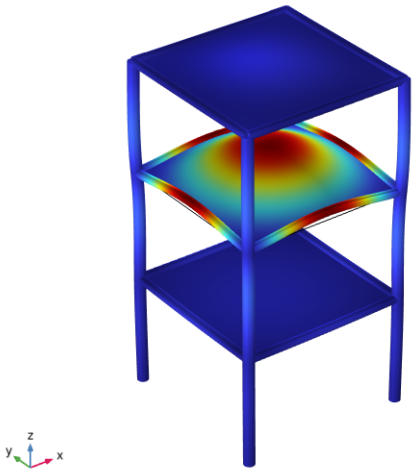

(b) *Second vertical mode of vibration,* $f = 10.02Hz$

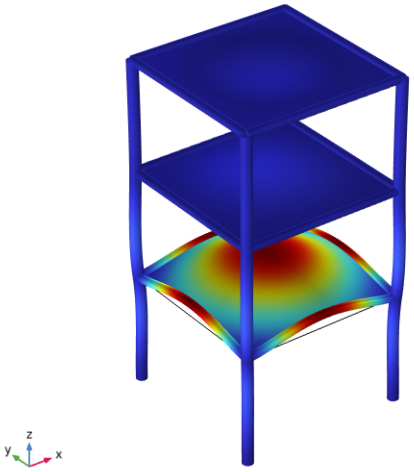

(c) *Third vertical mode of vibration,* $f = 11.93Hz$

Figure 5.4: *First three vertical modes of vibration of the building*

Here, a table with the eigenfrequencies relative to the first three sway modes of vibration and to the first three vertical modes of vibrations is reported:

Eigenfrequency [Hz]	Angular frequency [rad/s]	Damping ratio [-]	
2.29+0.05i	14.39+0.29i	0.02	Sway mode 1
7.80+0.16i	48.99+0.98i	0.02	Vertical mode 1
7.97+0.16i	50.03+1.00i	0.02	Sway mode 2
10.02+0.20i	62.96+1.26i	0.02	Vertical mode 2
11.93+0.24i	74.94+1.50i	0.02	Vertical mode 3
16.33+0.33i	102.58+2.05i	0.02	Sway mode 3

Table 5.1: *Eigenfrequency of the building on fixed constraints*

As clearly noticeable, the value of the eigenfrequency is a complex number. This is due to the fact that the material damping has been considered for the materials that compose the building.
As long the steel and the concrete have been thought to have the same damping ratio, for all the eigenfrequencies the value of the damping associated to that mode of vibration is 2%.
This is given by the fact that the building is fixed, so the radiation damping of the soil does not affect the results. This is because in this stage the radiation damping has not been taken into count.

5.2 Soil

The soil domain has been modeled according to these assumptions :

- one layer of soil lying on bedrock;
- interface between soil and bedrock fully horizontal.

As stated before, different models of the soil domain have been created, with different dimensions, depending on the aim of the model.
Despite the different dimensions, the "big" model and the "small" model have a lot in common, because they represent the same type of soil.
The dimensions of the big model, shown in Figure 5.5(a), used to compute the reference solution, which contains also the building, modeled as described in Section 5.1, are $13m$ in x direction, $13m$ in y direction and $7.5m$ in z direction, providing a space between the centers of foundation groups of $6m$.
The dimensions of the small model of the soil domain, which contains just one foundation group and that has been used to compute the impedance of the foundation or

the displacement of the foundation when the external load is present, shown in Figure 5.5(b), are $6.5m$ in x direction, $6.5m$ in y direction and $7.5m$ in z direction.

In both cases of study, the soil is the same. The only difference is the type of foundation: both piles group foundation and slab foundation have been studied.
The type of soil that has been chosen is soft soil, as common in Sweden, so the piles foundation represents a practical situation, while the slab foundation is just a theoretical case.
The parameters that characterize the soil are:

- Young's modulus $[Pa] = 18270000$
- Poisson ratio $[-] = 0.45$
- Density $[kg/m^3] = 1750$
- Damping ratio $[\%] = 5$
- Shear wave velocity $[m/s] = 60$
- Pressure wave velocity $[m/s] = 199$

The computational domain, which has the dimensions cited above, is surrounded by a PML domain with a thickness of $2m$.
As long the soil is supposed to lay on bedrock, the PML domain is present just around the soil domain and not at the bottom. This is due to the fact that, not being the case of study an halfspace, the reflection of the waves given by the bedrock has to be taken in count.
The stretching function used for the PML is the one described by equation 3.16 in section 3.3. The parameters that have been chosen, after a series of trials and convergence of results, are: $f_0^e = f_0^p = 10$.
The external boundaries of the PML domain, such as the bottom face of the computational domain, have been constrained with a fixed constraint, while the top surface of the model is free.
In the case of the slab foundation, it has been modeled just partitioning the computational domain and assigning to the partition surface located in the middle of the domain, which has dimensions $1.7m$ in x direction and $1.7m$ in y direction, a massless

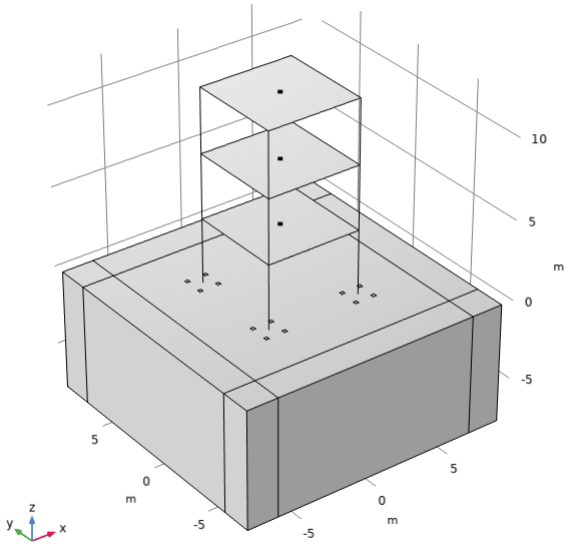

(a) *3D FEM-PML big model of soil, building and foundation*

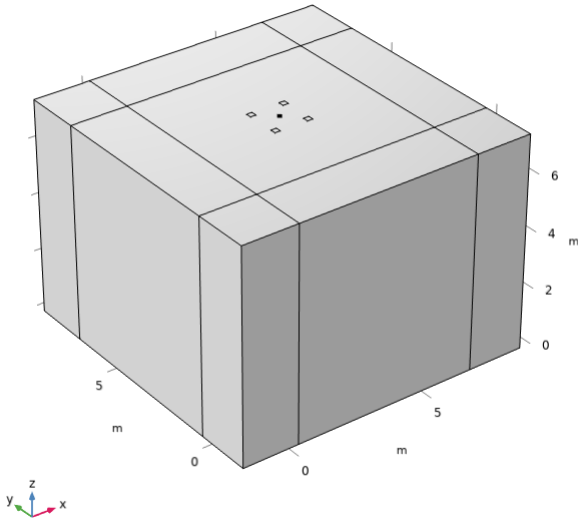

(b) *3D FEM-PML small model of soil with just one foundation group*

Figure 5.5: *Big 3D FEM-PML model of the soil with building and all four foundation groups (a) and small 3D FEM-PML model of the soil with just one foundation group (b)*

rigid connector. This rigid connector guarantees the continuity in displacements of the foundation.
In the case of piles group foundation, the piles have been modeled as blocks embedded in the soil, having the following properties:

- Young's modulus $[Pa] = 30000000000$
- Poisson ratio $[-] = 0.25$
- Density $[kg/m^3] = 2500$
- Damping ratio $[\%] = 0.005$
- Edge of the squared piles $[m] = 0.2$
- Spacing between center of piles $[m] = 1.7$

The piles have been considered to be end-bearing piles, so their bottom face has been modeled as fixed.
As stated in [reference], in order to ensure that the finite element program "catches" exactly the wave, there have to be at least 12 nodes per wavelength.
As the wavelength is described as

$$\lambda = \frac{V_s}{f_{max}} \tag{5.1}$$

where λ is the wavelength, $V_s = 60m/s$ the shear wave velocity, and $f_{max} = 30Hz$ the maximum frequency of interest, then its value will be $2m$.
In the case of the utilization of a linear discretization field for the elements of the mesh of the soil, as shown in Figure 5.6(right), we need 12 elements to have 12 nodes. This means that in this case, the maximum size of the elements composing the mesh has to be $0.16m$.
In the case of the utilization of a quadratic discretization field for the elements of the mesh of the soil, as shown in Figure 5.6(left), we need 6 elements to have 12 nodes; this means that in this case, the maximum size of the elements composing the mesh has to be $0.33m$.

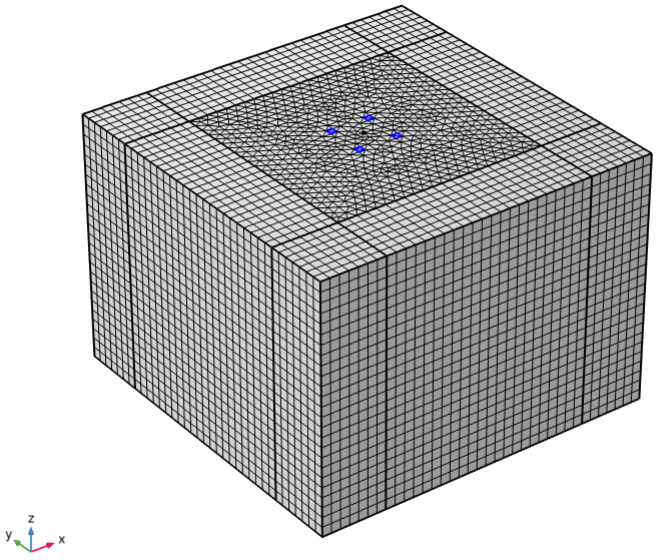

(a) *Mesh of the domain with quadratic displacement field discretization*

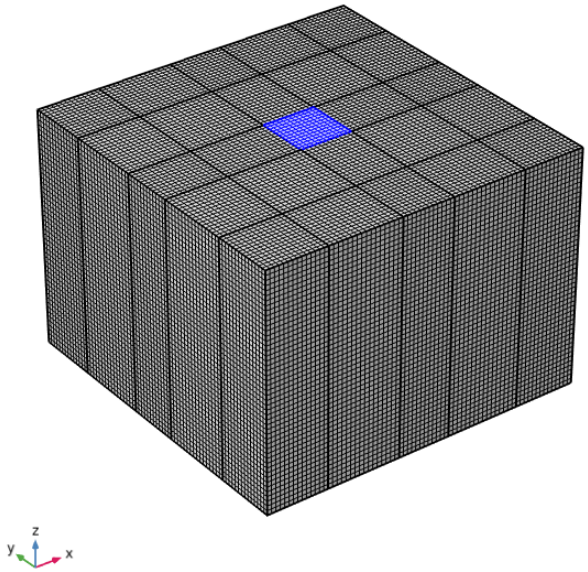

(b) *Mesh of the domain with linear displacement field discretization*

Figure 5.6: *Small 3D FEM-PML model of the soil with one piles group foundation showing quadratic discretization of the mesh elements (a) and small 3D FEM-PML model of the soil with one slab foundation showing linear discretization of the mesh elements (b)*

In the case of the slab foundation, the elements have been chosen to have a squared shape, because the geometry allows to make this choice.
In the case of the piles group foundation, instead, a triangular shape has been chosen for the elements, in order to have a more equal distribution of the elements around the piles groups.
For the PML domain, the elements are always squared, due to its dependence on Cartesian coordinates.

5.2.1 Comparison with literature results

In order to check if the modeling strategy that has been adopted is valid and that the PML domain works properly, a comparison between the results obtained for the vertical impedance of a piles group with a circular cross-section over bedrock and the result present in the literature ([14]) has been performed.
For what regards the slab foundation, the comparison has been done with point values of the vertical impedance of a slab over half space and the theoretical values that have been found in the literature ([20]).
In both cases, the results are related to the same type of soil considered in the literature reference ([14]), which has the following properties:

- Young's modulus $[Pa] = 386000679.6$
- Poisson ratio $[-] = 0.4$
- Density $[kg/m^3] = 1750$
- Damping ratio $[\%] = 5$
- PML width $[m] = 2$
- Soil dimensions: $6.5m * 6.5m * 7.5m$
- Shear wave velocity $[m/s] = 280.67$
- Pressure wave velocity $[m/s] = 687.5$

and, for what regards the piles:

- Young's modulus $[Pa] = 38.6 \cdot 10^9$

- Poisson ratio $[-] = 0.25$
- Density $[kg/m^3] = 2500$
- Damping ratio $[\%] = 0$
- Edge of the squared piles $[m] = 0.5$
- Spacing between center of piles $[m] = 2.5$

The shear wave velocity is $V_s = 280.6m/s$, and the maximum frequency of interest, in order to get the adimensional frequency $a_0 = \frac{\omega L_s}{V_s}$ equal to 1 is $f_{max} \approx 23Hz$. Therefore, the wavelength would be equal to $12m$. This means that the maximum size of an element with a linear displacement field discretization is $1m$.
The choice has been to limit the maximum size of the element to $0.45m$, because in this case, the restriction given by the need for twelve nodes per wavelength is not dominant.

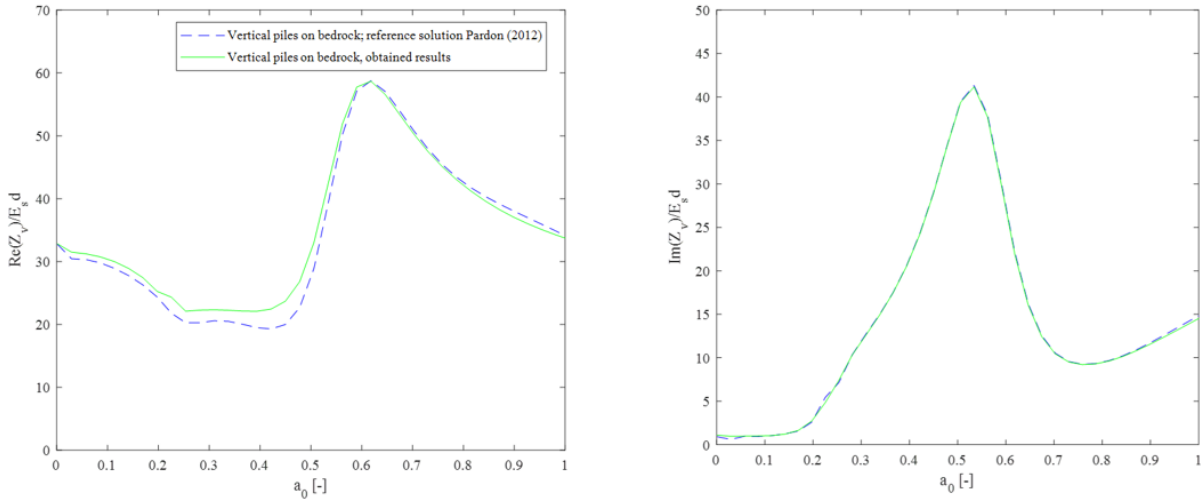

Figure 5.7: *Comparison between obtained results for vertical impedance and results from [14], real part (left) and imaginary part (right), both divided by a normalization factor*

In Figure 5.7, a comparison is presented between the obtained results for vertical impedance in the discussed case of pile foundations and those found in the literature ([14]). Both the Real and Imaginary parts of the impedance are normalized by a factor where E_S represents the Young's modulus of the soil, and d represents the spacing

between the center of the piles. These values are then plotted against the dimensionless frequency $a_0 = \frac{\omega L_s}{V_s}$, where ω represents the circular natural frequency, L_s is the thickness of the PML domain, and V_s is the shear wave velocity of the soil.

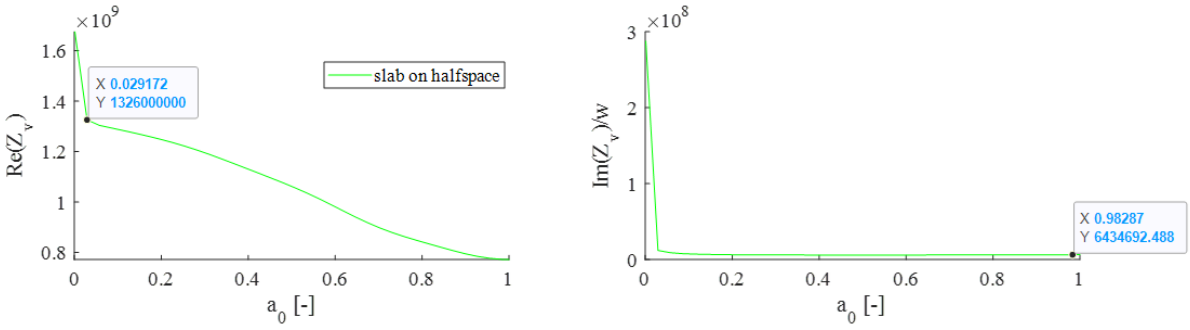

Figure 5.8: *Vertical impedance fo slab on half-space; dynamic stiffness (left) and damping (right)*

Figure 5.8 shows the results for vertical dynamic stiffness (left) and damping (right) for the slab foundation over half-space described above, plotted against the adimensional frequency a_0.
The values obtained at $a_0 \approx 0$ in the case of the stiffness and $a_0 \approx 1$ in the case of the damping have been compared with the ones coming from analytical formulas from literature ([12]):

$$k_{v,half}(0) = \frac{\rho V_s^2 A_f}{2B(1-\nu)} \cdot (0.73 + 1.54(\frac{B}{L})^{3/4} \tag{5.2}$$

for what concerns the stiffness and

$$c_{v,half}(1) = \rho V_{La} A_f \tag{5.3}$$

for what concerns the damping; where B and L are the half of the side dimensions of the slab foundation, A_f is the area of the slab foundation, ρ is the density of the soil, V_s is the shear velocity of the soil, ν is the Poisson ratio of the soil and $V_{La} = \frac{3.4 V_s}{\pi(1-\nu)}$ is the Lysmer's analog wave velocity ([7]).

With the values of those parameters described above, the results coming from the equations 5.2 and 5.3 are:

$$k_{v,half}(0) = 1303901105N/m$$

and

$$c_{v,half}(1) = 6110326,68Ns/m$$

As noticeable, the results obtained from the model are quite similar tho the ones obtained with equations 5.2 and 5.3. In the case of the stiffness, the percentual error with respect to the theoretical solution is 1.6%, while in the case of the damping, it is 5.3%.

Chapter 6

Results

In this chapter, the results obtained through the analysis using the method under study are presented and compared with those obtained by modeling both the soil and the building, representing the reference solution.
Initially, the dynamic stiffness and damping, obtained by computing the foundation impedance, are plotted.
Following that, changes in eigenfrequencies related to the building's vertical motion are shown.
Subsequently, velocities of the floors are displayed, obtained by directly applying a load to the first floor of the building. These results helps highlight the frequency response peaks linked to vertical modes of vibrations and demonstrates the effectiveness of the spring and dampers in approximating the soil.
Next, a comparison is made between foundation displacements when the load is applied 12 meters from the center of the rigid connector, illustrating the influence of neighboring foundations.
Finally, a comparison is presented between the reference solutions and the results obtained with the method under study. The effects on the results of the introduction of phase shift and coupling terms in impedance is discussed.

6.1 Impedances

In this section, the results of the impedance computed for the two cases of study are shown.

The impedance has been computed for a single foundation. The assumption that the presence of other foundation groups in the surroundings does not affect the results has been done.

Both for pile group foundations and slab foundations, a symmetry exists because the foundation has identical dimensions along the x and y axes. Due to this symmetry in both the computational domain and the foundation, the sway and rocking terms have been computed only once. This is because the results are identical, given the symmetry of the setup.

With the aim of a better understanding of the results shown presented in Subsections 6.1.1 and 6.1.2, a schematization of the unitary applied displacements. The correspondent reaction forces and moments is shown in Figure 6.1.

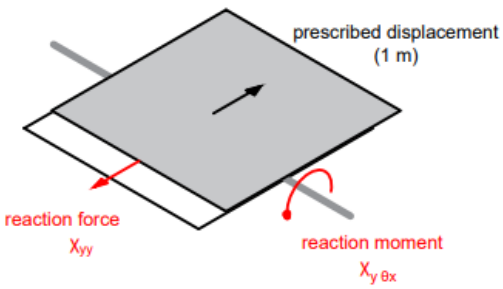

(a) *Direct term χ_{yy} and coupling term $\chi_{y\theta_x}$ of the impedance matrix*

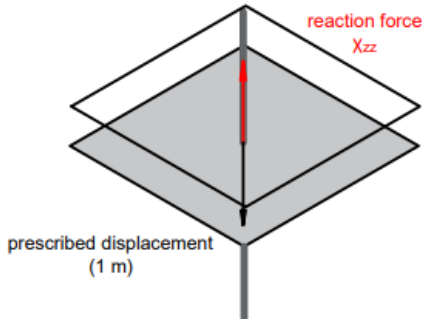

(b) *Direct term χ_{zz} of the impedance matrix*

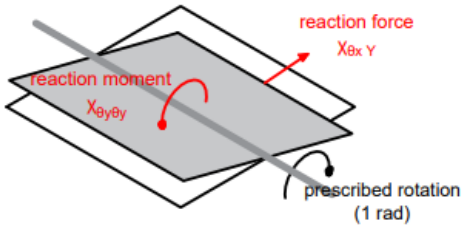

(c) *Direct term $\chi_{\theta_y\theta_y}$ and coupling term $\chi_{\theta_x y}$ of the impedance matrix*

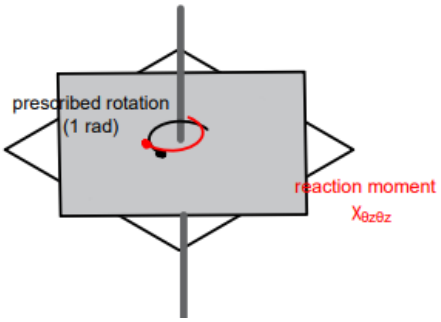

(d) *Direct term $\chi_{\theta_z\theta_z}$ of the impedance matrix*

Figure 6.1: *Schematization of the computation of the terms of the impedance matrix of a slab foundation*

6.1.1 Slab foundation

In Figure 6.2 and 6.3, are shown the direct terms of the impedances. These terms are the ones located on the diagonal in the impedance matrix (Equation 3.22).
On the left is shown the dynamic stiffness, while on the right is the damping.

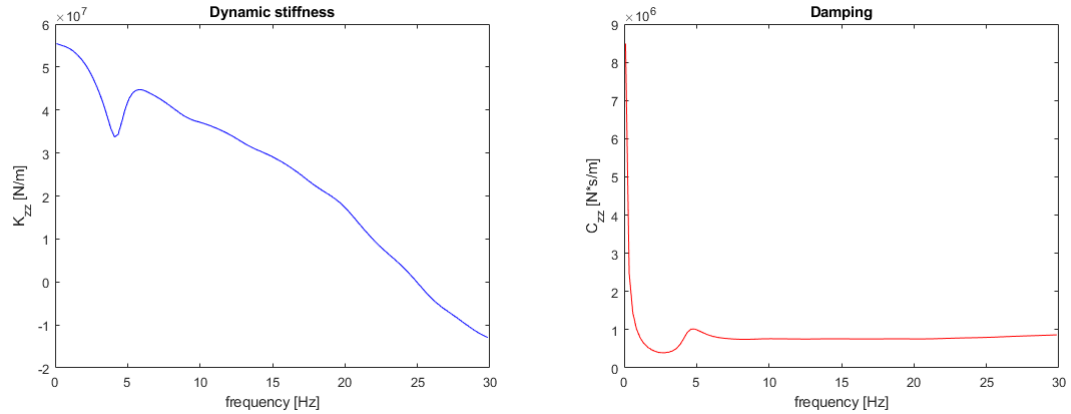

(a) K_{zz}

(b) C_{zz}

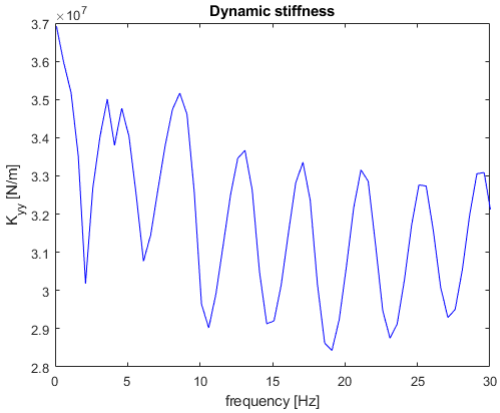

(c) K_{yy}

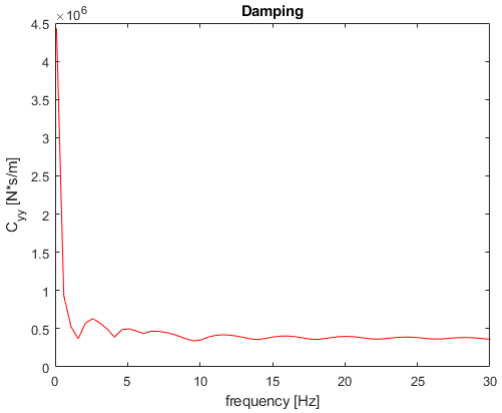

(d) C_{yy}

Figure 6.2: *Sway terms of the impedance function of a slab foundation on soft soil, dynamic stiffness in blue (left) and damping in red (right). For a better understanding of the various terms, refer to Figure 6.1*

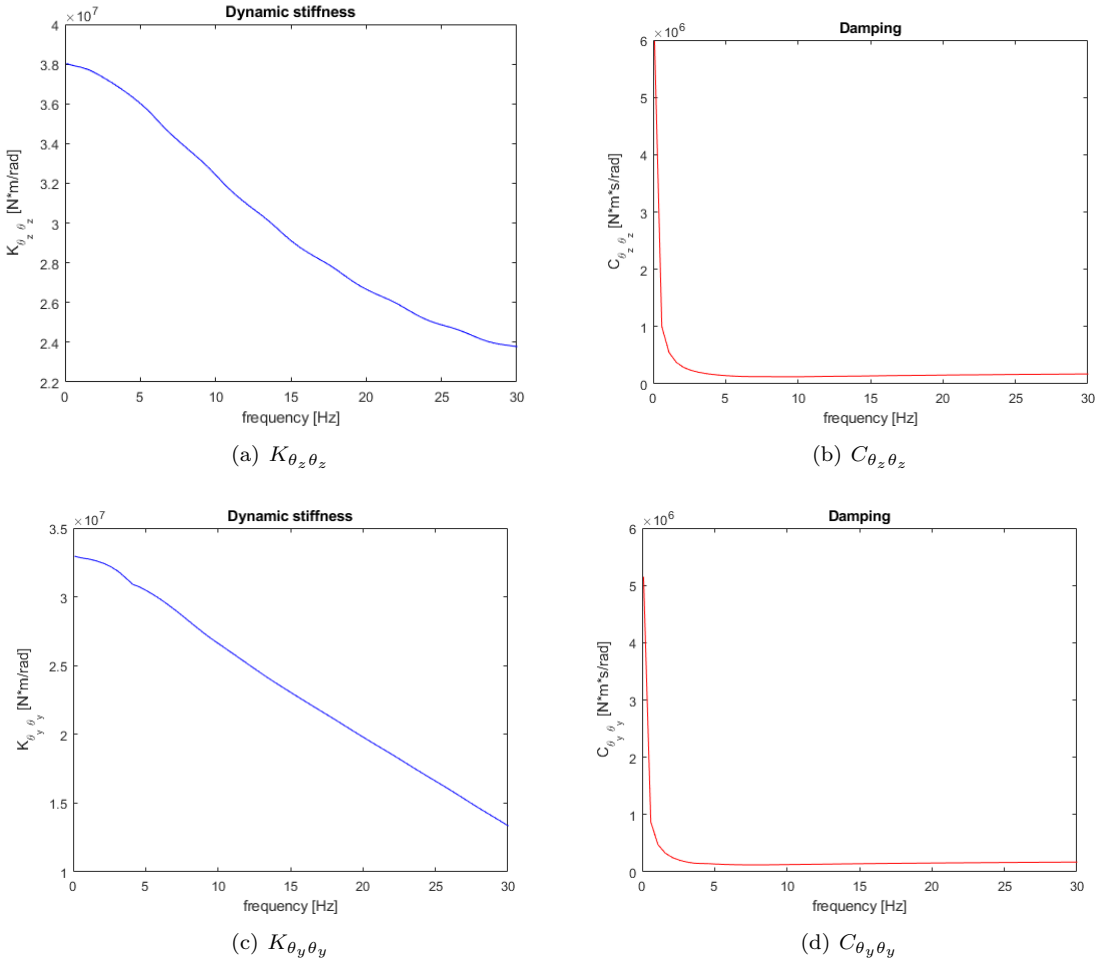

(a) $K_{\theta_z\theta_z}$ (b) $C_{\theta_z\theta_z}$

(c) $K_{\theta_y\theta_y}$ (d) $C_{\theta_y\theta_y}$

Figure 6.3: *Rocking terms of the impedance function of a slab foundation on soft soil, dynamic stiffness in blue (left) and damping in red (right). For a better understanding of the various terms, refer to Figure 6.1*

As appreciable from the plots of Figures 6.2 and 6.3, especially in the case of the dynamic stiffness related to the vertical sway, the stiffness shows a drop at the natural frequency of the soil, evaluated as:

$$f_c \approx \frac{V_{La}}{4H} \approx 4Hz \tag{6.1}$$

As expected, the values of the impedance concerning the vertical sway are higher than all the others.

Also, is clearly visible as the horizontal sway has really oscillating values for different

frequencies, while all the other stiffnesses tend to decrease when the frequency gets higher.
After an initial drop, the value of the damping remains constant for all the cases.
In the case of the coupling terms of the impedance, the results are shown in Figure 6.4.

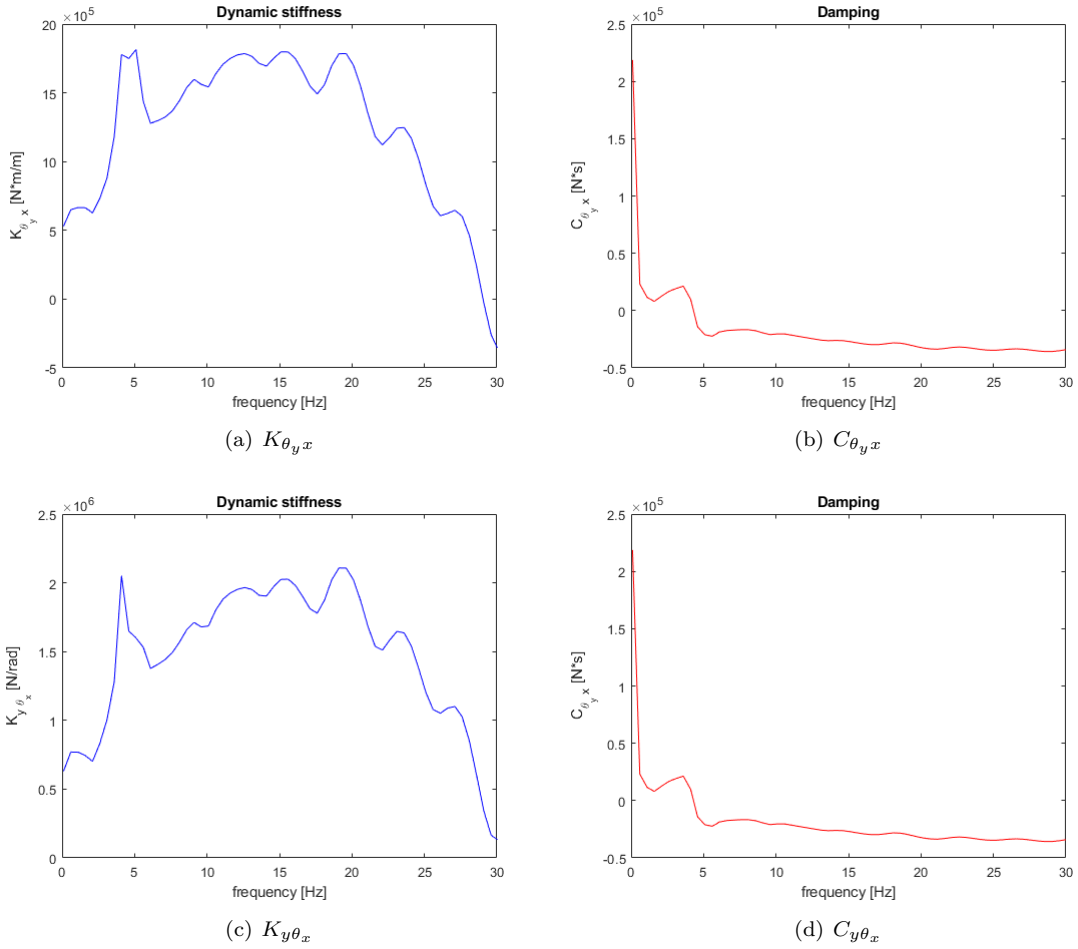

(a) $K_{\theta_y x}$ (b) $C_{\theta_y x}$

(c) $K_{y\theta_x}$ (d) $C_{y\theta_x}$

Figure 6.4: *Coupling terms of the impedance function of a slab foundation on soft soil, dynamic stiffness in blue (left) and damping in red (right). For a better understanding of the various terms, refer to Figure 6.1*

Also here, for the symmetry of the foundation, these terms have been computed just along one direction.
Also, if compared, the results in the two cases are really close to each other, as expected, because of the symmetry property of the impedance matrix.

6.1.2 Piles group foundation

In Figure 6.5 and 6.6, are shown the direct terms of the impedances in the impedance matrix located on the diagonal.
On the left is shown the dynamic stiffness, while on the right the damping.

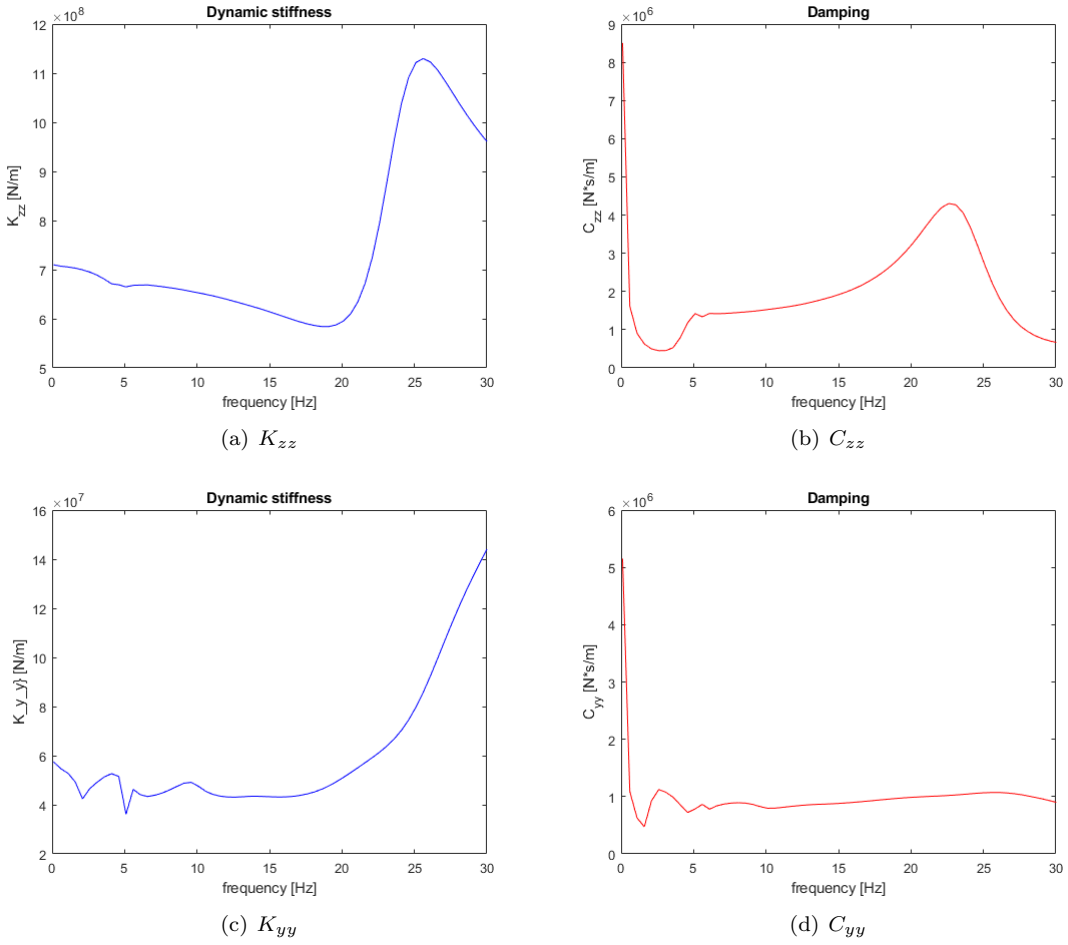

(a) K_{zz} (b) C_{zz}

(c) K_{yy} (d) C_{yy}

Figure 6.5: *Sway terms of the impedance function of an end-bearing piles group foundation on soft soil, dynamic stiffness in blue (left) and damping in red (right). For a better understanding of the various terms, refer to Figure 6.1*

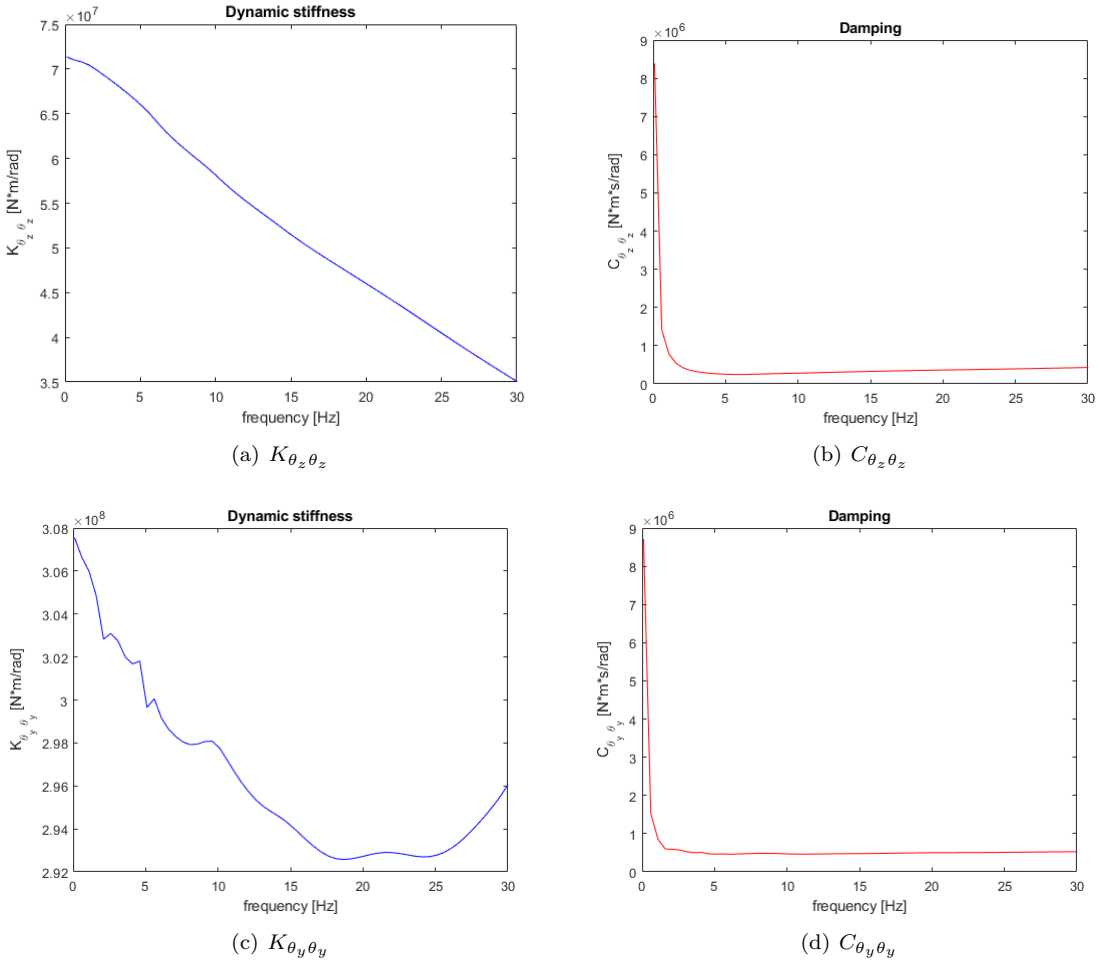

(a) $K_{\theta_z\theta_z}$ (b) $C_{\theta_z\theta_z}$

(c) $K_{\theta_y\theta_y}$ (d) $C_{\theta_y\theta_y}$

Figure 6.6: *Rocking terms of the impedance function of an end-bearing piles group foundation on soft soil, dynamic stiffness in blue (left) and damping in red (right). For a better understanding of the various terms, refer to Figure 6.1*

As appreciable from the plots of Figures 6.5(a) and 6.5(b), a flex in the dynamic stiffness and a peak in the damping is present at the natural frequency of the pile group foundation.

As expected, the values concerning the vertical sway are higher than all the others, of one order of magnitude when compared to the horizontal sway impedance.

After an initial drop, the value of the damping remains constant for all the cases, apart from the one of the vertical sway, where a peak at the natural frequency of the pile group is present.

In the case of the coupling terms of the impedance, the results are shown in Figure 6.7.

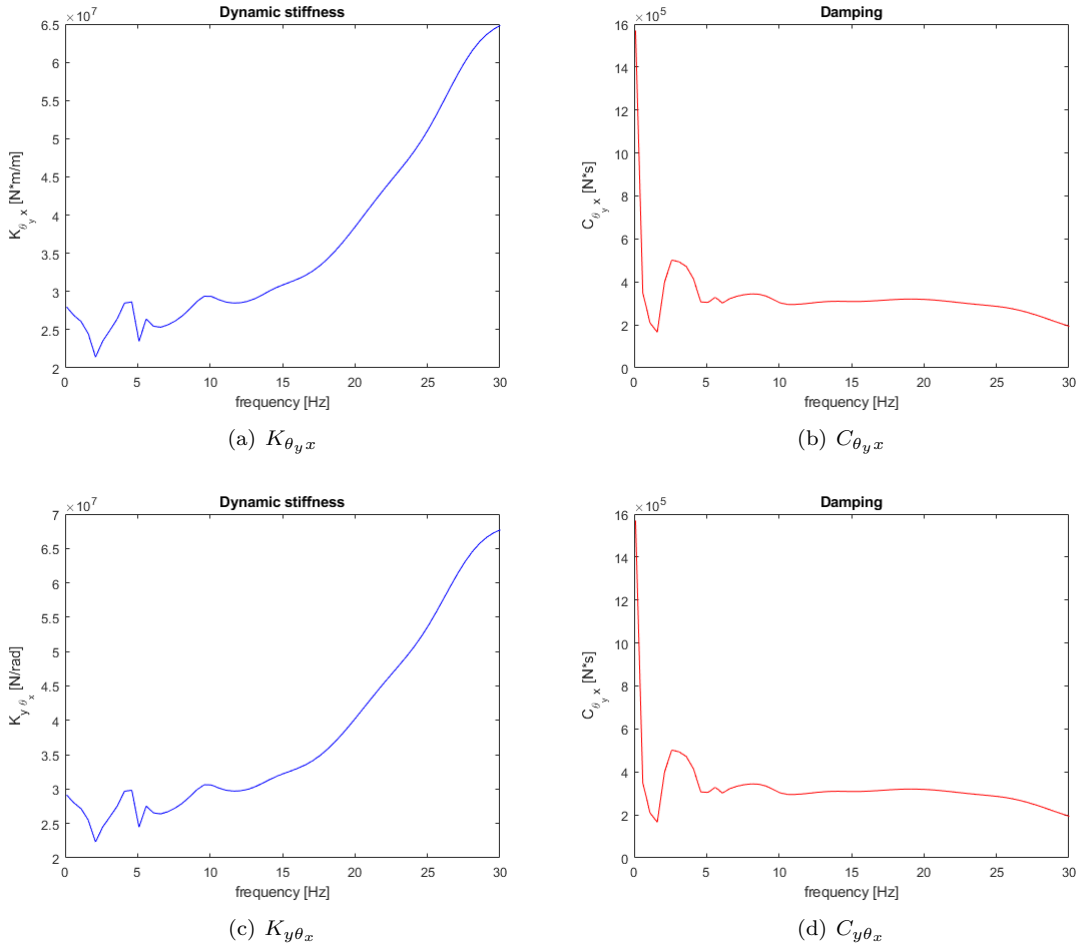

(a) $K_{\theta_y x}$ (b) $C_{\theta_y x}$

(c) $K_{y\theta_x}$ (d) $C_{y\theta_x}$

Figure 6.7: *Coupling terms of the impedance function of a an end-bearing piles group foundation on soft soil, dynamic stiffness in blue (left) and damping in red (right). For a better understanding of the various terms, refer to Figure 6.1*

Also here, for the symmetry of the foundation, these terms have been computed just along one direction.

Also, if compared, the results in the two cases are really close to each other, as expected, because of the symmetry property of the impedance matrix.

6.2 Eigenfrequency change

When the building is modeled with spring and dashpots at its foundation that simulate the impedance, its eigenfrequency changes. This is given by a change in stiffness and damping with respect to to case with fixed ends and also by the lumped mass at the bottom of the column oscillates, while in the case with fixed constraints it doesn't.
This new eigenfrequencies have been computed by applying in a first step the impedance relative to the natural frequency of the fixed building and, once run the eigenfrequency analysis and found the new eigenfrequency, the impedance relative to this new value has been introduced. This procedure has been iterated until convergence, separately for all first three vertical modes of vibration of the building.
In the tables 6.2 and 6.2 this eigenfrequency change is shown.

Eigenfrequency [Hz]	Damping ratio [-]		Eigenfrequency [Hz]	Damping ratio [-]
7,80+0,16i	0,02	→	8.21+0.29i	0.035
10,02+0,20i	0,02	→	10.50+0.37i	0.035
11,93+0,24i	0,012	→	15.20+1.60i	0.104

Table 6.1: *Change in eigenfrequency of the building over spring and dashpots simulating slab foundations*

Eigenfrequency [Hz]	Damping ratio [-]		Eigenfrequency [Hz]	Damping ratio [-]
7,80+0,161i	0,02	→	7.72+0.16i	0.021
10,02+0,20i	0,02	→	9.80+0.22i	0.023
11,93+0,24i	0,02	→	11.36+0.41i	0.036

Table 6.2: *Change in eigenfrequency of the building over spring and dashpots simulating end bearing piles groups foundations*

The change in the eigenfrequencies of the building is different in the two cases. For what concerns the building on piles, the three eigenfrequencies become slightly lower, while in the case of building on slab, the value of the eigenfrequencies increases of a non-negligible quantity.
Taking in consideration the damping ratio, instead, both cases follow the same trend. The damping ratio increases due to the radiation damping given by the presence of the impedance. For the building on slabs this rise of the value of damping is greater.

6.3 Comparison between slab displacements and SDoF

To assess the efficiency and reliability of introducing impedance functions coupled with displacements as the base motion, a comparison is conducted. The comparison involves examining the displacements on a slab foundation when subjected to a load applied 12 meters from its center. This is compared to a single-degree-of-freedom system, where the system's mass is equivalent to the mass of the slab. The spring constant in this system corresponds to the vertical dynamic stiffness of the soil-foundation system. The dashpot coefficient represents the vertical damping of the soil-foundation system. The perturbation is introduced through free-field displacements computed on the same soil model without the presence of the slab foundation.

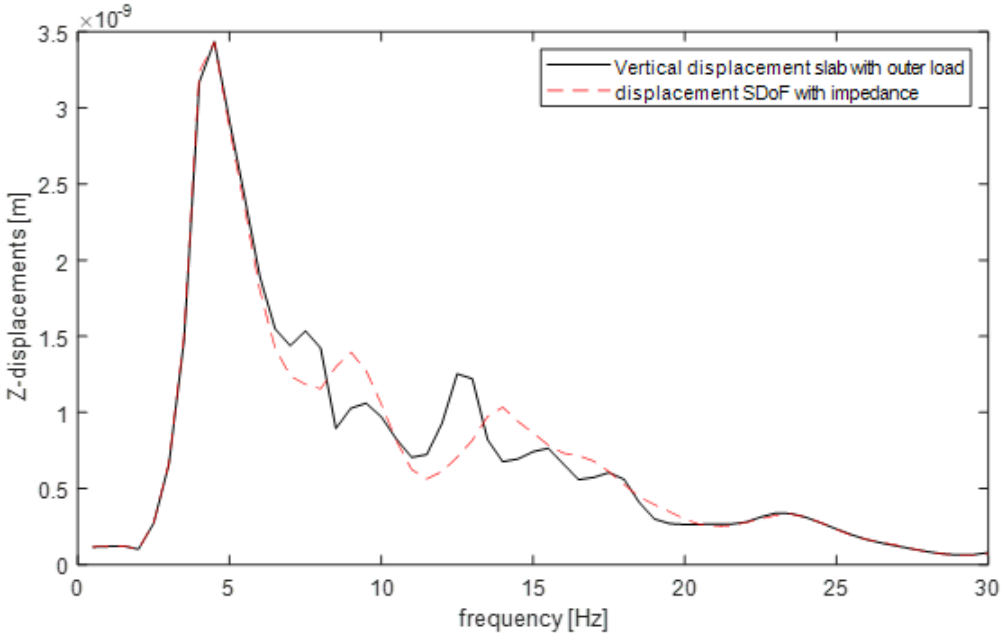

Figure 6.8: *Comparison between the displacement of the foundation and a single degree of freedom system simulating the foundation*

Figure 6.8 show the comparison between the slab foundation and the single degree of freedom system that represents that foundation.
The results coincide for what regards high frequencies and most of all for the frequency

that represents the natural frequency of the soil and in which the displacement function shows a peak.
The disparities in the middle frequencies can be attributed to two primary reasons. Firstly, in the single-degree-of-freedom system, only the vertical impedance has been incorporated, without accounting for any other sway or rocking terms. Secondly, the analysis of the slab is conducted within a 3D environment, allowing for displacements in all directions. In contrast, the single-degree-of-freedom system represents a point, symbolized by a lumped mass, capable of displacements in just one direction and without rotations.
Those differences, despite those discrepancies between the models, are not that marked. The fact that on the peak corresponding to the resonance of the soil domain the two solutions coincide indicates that the way in which the impedances are introduced, with the aim to simulate the role of the foundation in the soil, works.

6.4 Velocities of floors due to a load applied on the building

In this section, a plot of the velocities of the floors of the building is purposed. This has been made to visualize the position of the peaks in the frequency domain, situated at the same frequencies shown in the section 6.2. Also, this computation proofs that how the impedance has been applied under the building simulates in a good way the effect given by the presence of the soil under the building.
In both cases, a unitary load has as been applied on the first floor of the building and a frequency domain analysis has been run. The results taken are the velocities of the three floor slabs at their mid-point.

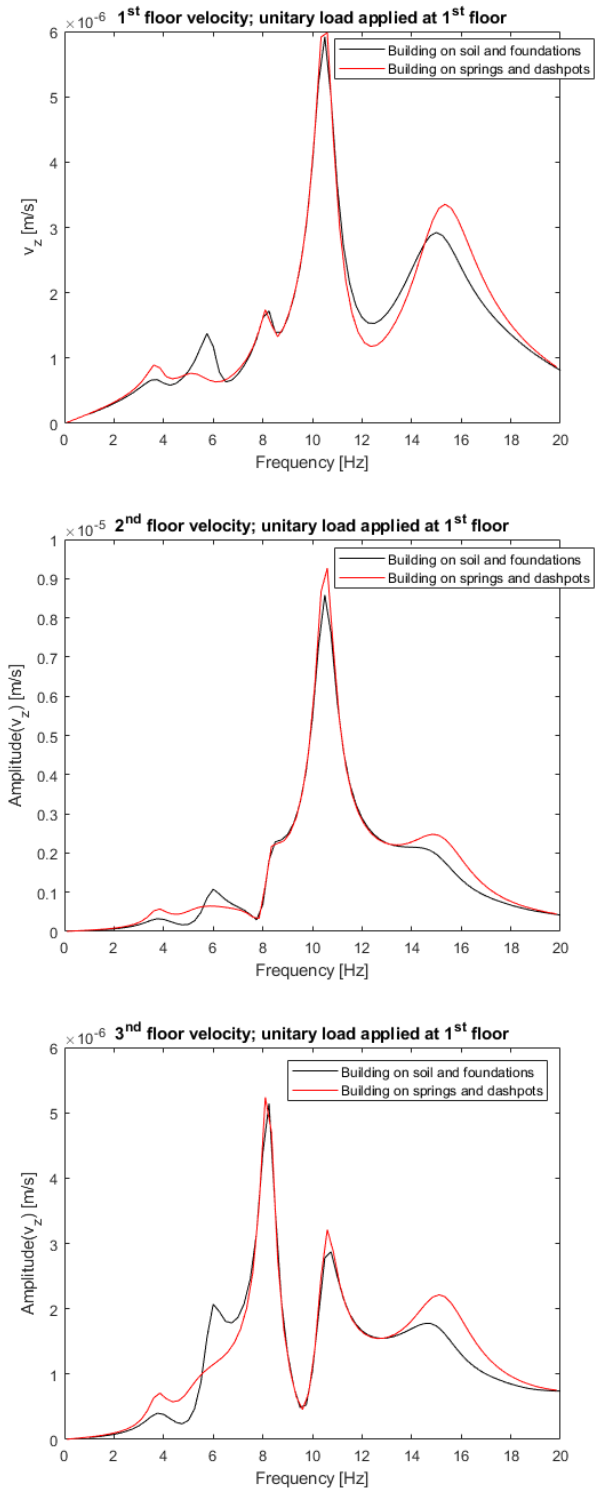

Figure 6.9: *Vertical velocity of the three floors of the studied building on slab foundation when a unitary load is applied at the first floor*

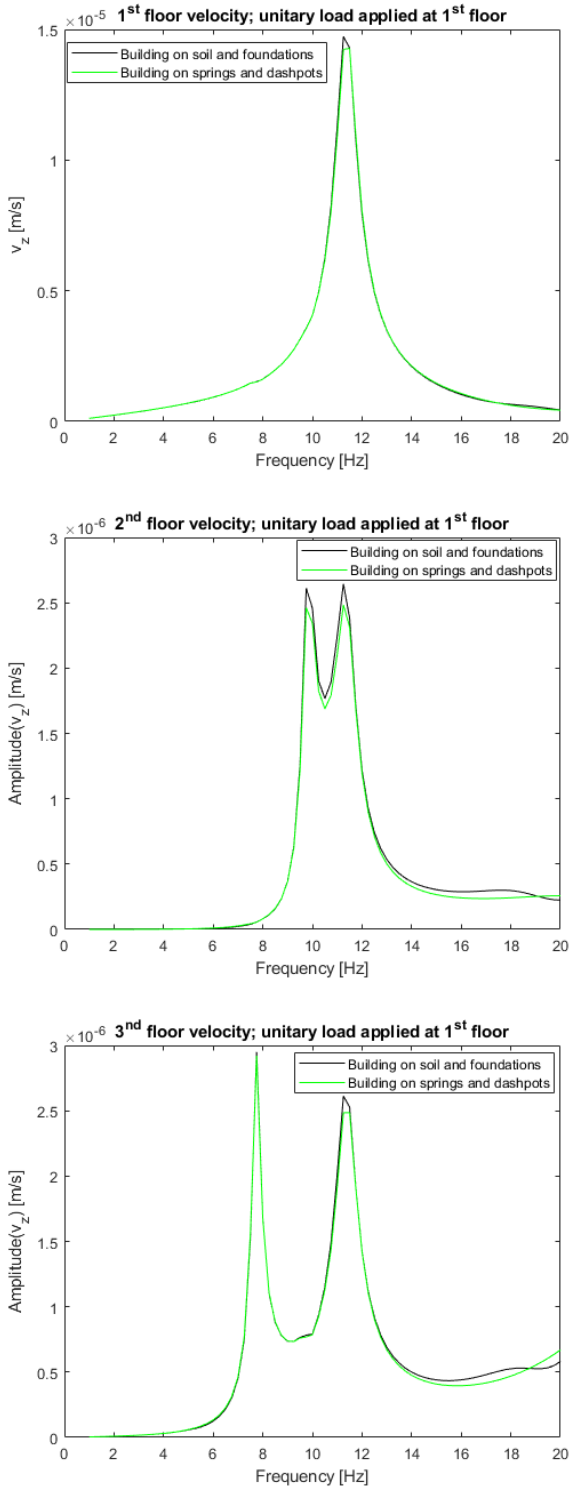

Figure 6.10: *Vertical velocity of the three floors of the studied building on piles group foundation when a unitary load is applied at the first floor*

As appreciable from figure 6.9 and 6.10, the value of the velocities at the peaks in the frequency domain is close. This indicates that the method used to introduce the impedances at the bottom of the building is reliable.

6.5 Displacements on foundations due to the external load

To compute the displacements for use as a base motion at the bottom of the building, a model featuring only one foundation was utilized. This model was subjected to a load positioned at distances of both 12 meters and 18 meters from the foundation center. This procedure was carried out for both pile group and slab foundations, as detailed in Section 4.3.3.
The displacements obtained from the analysis when the load was placed 12 meters from the foundation center were compared with the displacement values computed by applying an external load situated 15 meters away from the center of a model containing all four foundation groups. This comparison aimed to assess the impact of the presence of other foundation groups in the vicinity.

Figure 6.11 shows a comparison of the displacements of the slab foundation when the model with four foundations and the model with just one foundation is excited by an external load that simulates the traffic, distant 12 m from the center of the foundation. The comparison for both horizontal and vertical displacements shows that the two approaches give almost the same results. Therefore, the presence of other slab foundations does not influence the displacements given by a distanced load.
There are some frequency intervals in which the results present differences. The ones computed on the model with just one foundation are higher when compared to the ones that come from the model with four foundations.

This is because, in the model with four foundations, the load is applied at 15 m from the center of the model and it is not centered with the foundations center. Due to this, the distance between the point of the application of the load and the closer foundation is not precisely 12 m, but slightly higher.
This brings to a small discrepancy in the computed displacements. This small difference can be considered not relevant for practical purposes, bringing to the assumption that

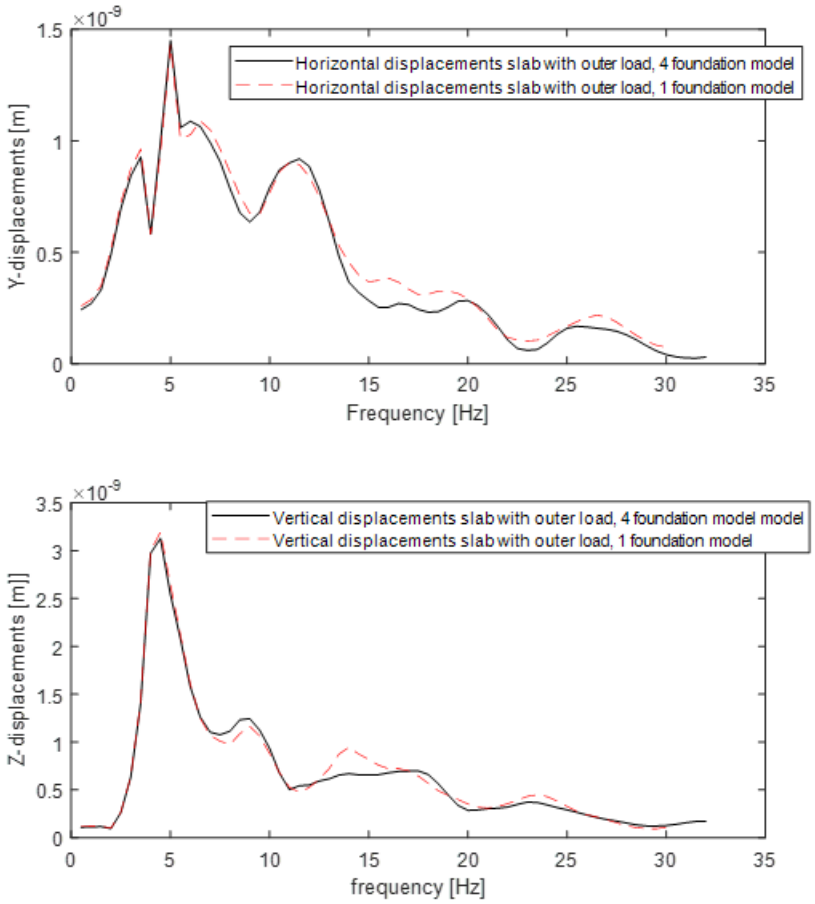

Figure 6.11: *Comparison between horizontal (top) and vertical (bottom) displacements of a slab foundation computed with a model with all the four foundations (black line) and with a model with just 1 foundation (red dashed line); in both the distance between the load and the center of the foundation is 12 m.*

the displacements computed on a small domain with just one foundation can be used as a base motion under the building.

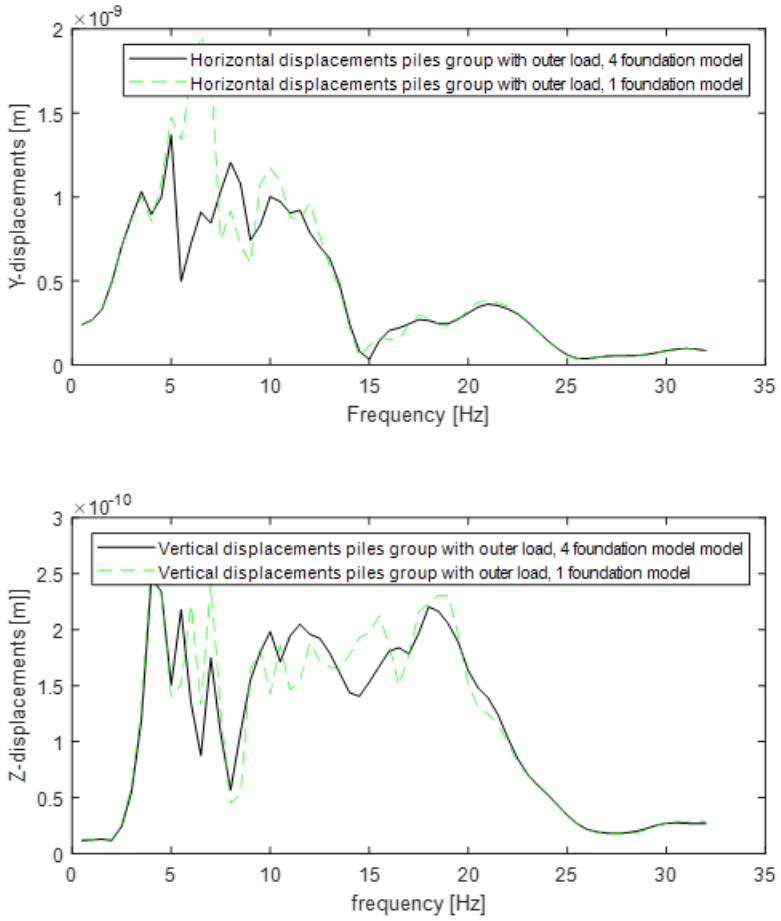

Figure 6.12: *Comparison between horizontal (top) and vertical (bottom) displacements of a pile group foundation computed with a model with all the four foundations (black line) and with a model with just 1 foundation (green dashed line); in both the distance between the load and the center of the foundation is 12 m.*

Figure 6.12 illustrates a comparison of the displacements for the pile group foundation when excited by an external load simulating traffic. The load is placed 12 meters away from the center of the foundation.
The comparison covers both horizontal and vertical displacements. The analysis reveals that the two approaches yield similar results for frequencies below $6Hz$ and those above

$20Hz$. However, significant differences emerge for frequencies falling between these two values.
This indicates that the presence of other pile groups when applying a traffic load has a noticeable influence on the results, and this influence cannot be disregarded. As a result, the displacements computed using the soil model with all four foundations have been employed as a base motion to obtain more precise results.
This influence of neighboring pile groups on displacement values also suggests that these groups can affect impedance values.
Furthermore, if there are other pile group foundations from neighboring buildings in the vicinity, their presence should be taken into consideration.

6.6 Velocities of floors due to the external load

Following the incorporation of springs and dashpots under the building, simulating the soil impedances and the displacements modeled as a base motion, an analysis of floor velocities was conducted. Initially, this analysis was carried out without introducing phase shifts and coupling terms. Subsequently, the analysis was repeated with the introduction of phase shifts and coupling terms to investigate their impact on the results.

6.6.1 Building on slab foundation

Concerning the building over slab foundation, being thought to be placed on soft soil, its response is characterized by a peak in frequency around the eigenfrequency of the soil. This can be visualized in figure 6.13.

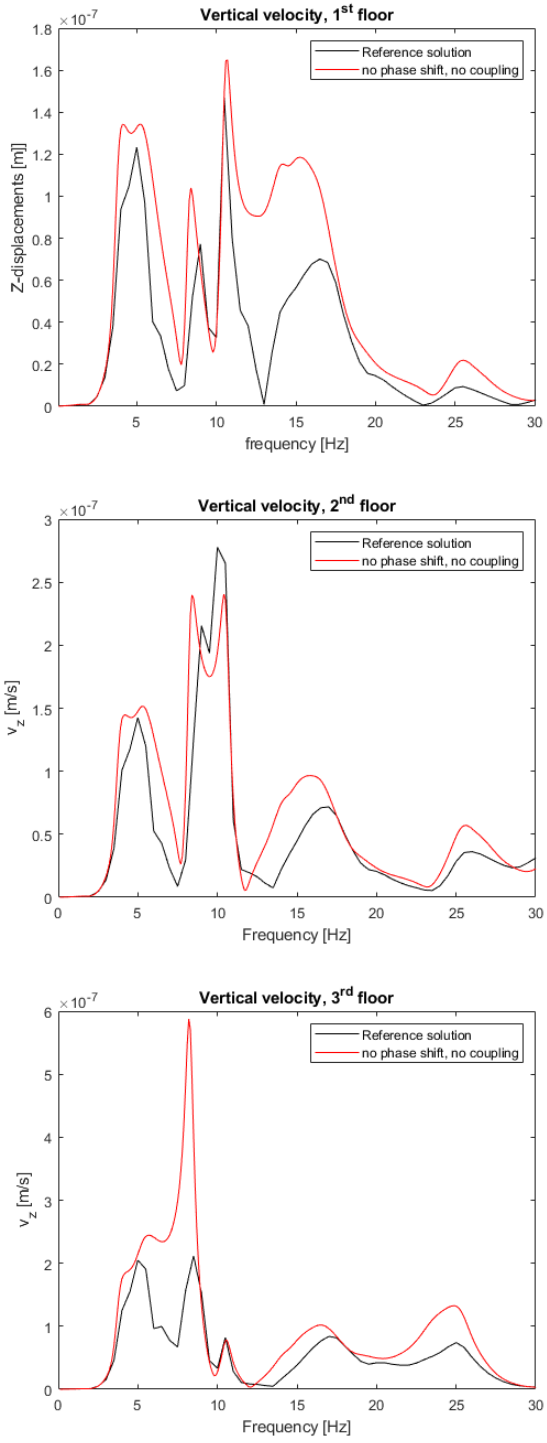

Figure 6.13: *Comparison between vertical velocities of the floors of the building obtained from the reference solution and by applying a base motion under the building on springs and dashpots; slab foundation.*

The initial computational method, which did not include the introduction of phase shifts and coupling terms in the impedance matrix, provided a reasonable approximation of the building's response around the natural frequency of the soil. However, this method was not as precise when it came to capturing the building's response at its own natural frequencies.
Despite the frequency peaks aligning with the new eigenfrequency of the building, the velocity values tended to be overestimated. For instance, this overestimation occurred in the first-floor velocity around $15Hz$ or in the velocity of the third floor around $8Hz$. When the phase shift was introduced, the results exhibited noticeable differences, as depicted in Figure 6.14.

As evident from Figure A.1 in Appendix A, the presence of coupling terms in the impedance matrix does not have a significant impact on the results.
Conversely, the introduction of a phase shift leads to a more accurate estimation of the vertical velocities of the floors at the eigenfrequency of the building.
Among the three different approaches to modeling the phase shift described in Subsection 4.3.4, the most reliable one is the method that involves multiplying the displacement amplitude by the cosine of the phase angle. This can be observed in Figure A.2 in Appendix A.
Upon examining Figure 6.14, it becomes evident that the peaks represented by the red plot are less precise compared to the ones described by the blue line when compared to the reference solution.
However, it's worth noting that when the phase shift is introduced in the base motion under the building, the peak in velocity related to the eigenfrequency of the soil is significantly underestimated.

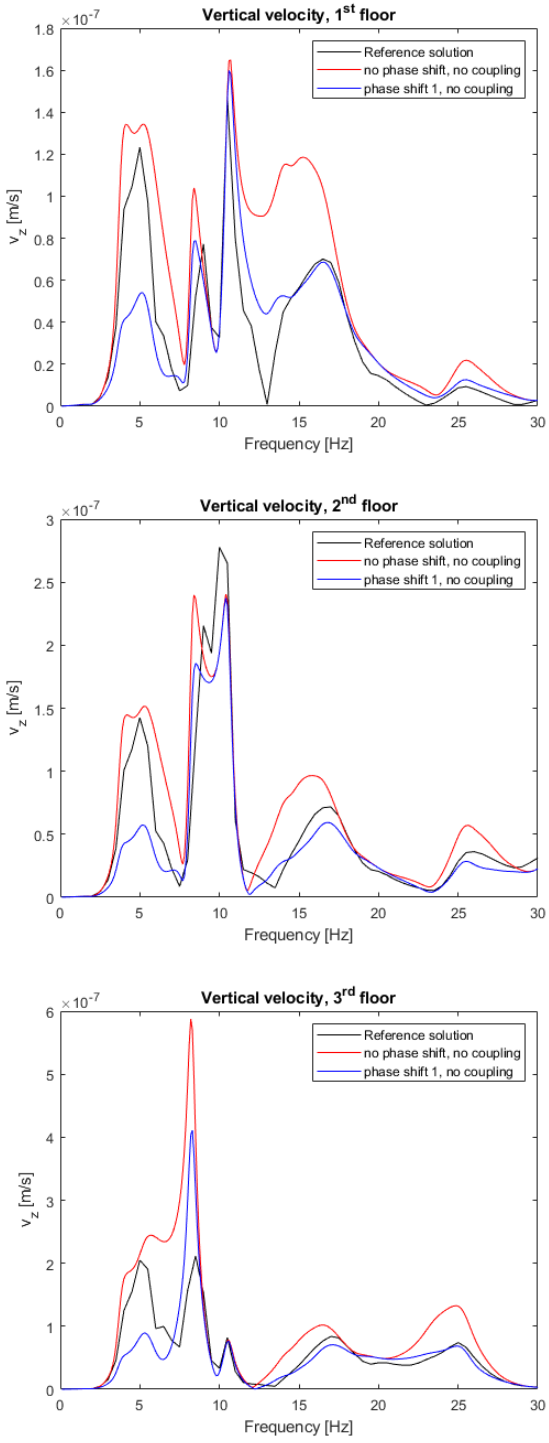

Figure 6.14: *Comparison between vertical velocities of the floors of the building obtained from the reference solution (black); by applying a basemotion under the building model with spring and dashpots without a phase shift (red); by applying a base motion under the building on springs and dashpots whit "phase shift 1"; slab foundation*

6.6.2 Building on piles group foundation

In the case of the building on piles foundation, the effect of the eigenfrequency of the soil on the building vibration is negligible.
This is given by the presence of the piles groups foundation. This type of foundation provides more stiffness to the system, ensuring lower displacements of the foundation when the soil domain goes under resonance and avoiding having a peak in the response relative to the natural frequency of the soil.
Another aspect that can be noticed by looking at figure 6.15, is that the peak around $18Hz$ is now greater, and another peak, around $24Hz$, appears in the third-floor velocity.
The results obtained show how, in the case of piles group foundation, the velocities of the building are really well approximated when this method is used, and most of the time are on the safe side.
The only bad comparison is present in the third-floor velocity, at the first eigenfrequency of the building. In this case, the velocity computed on the building and dashpots with an applied base motion is more than 4 times the one obtained from the reference solution.
Again, as in the case of the slab foundation, the introduction of the coupling terms in the impedance matrix does not affect the results. This can be appreciated by looking at Figure **??**, in Appendix A.
Between the three different modelling approaches concerning the phase shift described in Subsection 4.3.4, the most reliable one is the one that supposes the multiplication of the displacement amplitude by the cosine of the phase angle. This can be seen in Figure A.4, in Appendix A.
The introduction of the phase shift in the base motion refines the results. As is noticeable, in the graph concerning the velocity of the first floor in Figure 6.16, the peaks of the black line and the one of the blue line, that is the one describing the velocities of the building when the phase shift is taken in consideration, have the same value.
The introduction of phase shift helps also in having a reduction of the overestimated peak in the third-floor velocity. However, the difference between the reference solution and the building on spring and dashpots is high.
Also, despite the first three vertical frequencies of the building the results obtained

are quite precise and on the safe side, being higher than the ones obtained from the reference solution, for what regards the velocity of the third floor at $24Hz$, the obtained results are not very precise and they are not on the safe side.

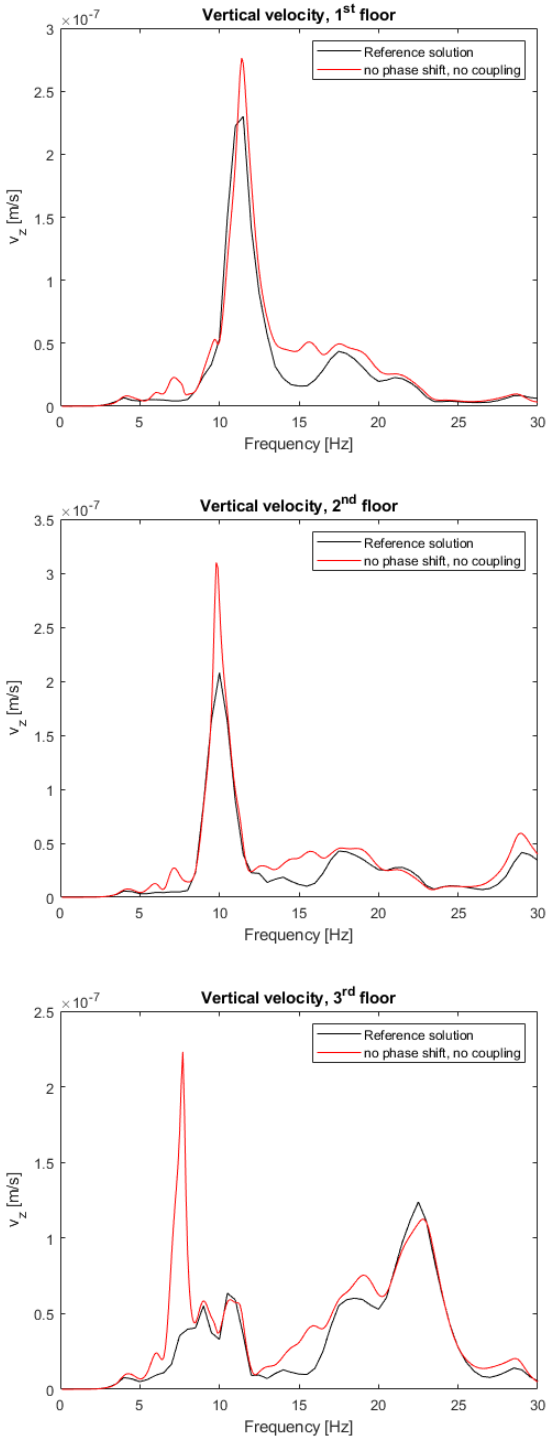

Figure 6.15: *Comparison between vertical velocities of the floors of the building obtained from the reference solution and by applying a base motion under the building on springs and dashpots; piles group foundation*

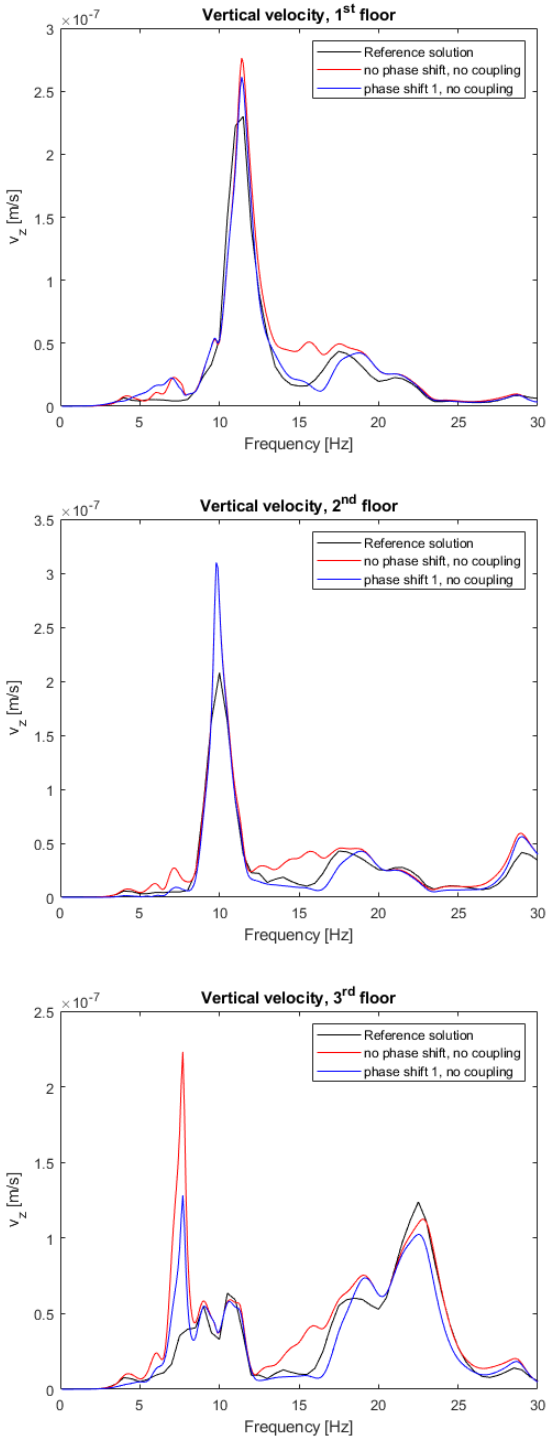

Figure 6.16: *Comparison between vertical velocities of the floors of the building obtained from the reference solution (black); by applying a basemotion under the building model with spring and dashpots without a phase shift (red); by applying a base motion under the building on springs and dashpots whit "phase shift 1"; piles group foundation*

Chapter 7

Conclusions

In this section, a final overview on the conducted research work on the numerical method to evaluate ground-born vibration on a building is purposed and the main conclusion are stated.

7.1 On the modeling approach

- As stated in section 3.3 and 5.2, the soil domain is very sensitive to the mesh size. This sensitivity arises because both the Perfect Matched Layer and the computational domain have maximum element size requirements. These requirements depend on the shear wave velocity of the soil and the maximum frequency of interest. The lower the shear wave velocity and the higher the maximum frequency of interest, the smaller the size of the element must be. This aspect significantly affects computational time.

- The parameters inserted in the stretching function for the PML require careful evaluation. These parameters should be well-suited in relation to the maximum frequency of interest. This evaluation is similar to the process applied to the mesh. The mesh needs to meet the requirement for maximum size to accurately capture the waves. Additionally, it should ensure continuity at the boundary between the computational domain and the PML.

- As shown in section 6.5, when it comes to slab foundations, the presence of other

slabs doesn't impact the computed displacements at the center of the foundation caused by an external load. However, for pile group foundations, this is not the case, especially concerning the frequency content associated with horizontal soil motion. In this context, the role of pile groups in terms of stiffening becomes significant. Consequently, a model that accounts for the presence of multiple pile groups must be used. This leads to an increased number of degrees of freedom in the model. As a result, there is a higher computational cost associated with such a model.

- Applying the values of the impedance functions under the building is a reliable approach. This approach treats them as a set of springs and dashpots. It effectively accounts for the effect of the soil, as demonstrated in Sections 6.3 and 6.4.

7.2 On the obtained results

- When applying base motion under the building without considering the phase shift between two distant foundations, the results generally err on the side of safety. However, there is a drawback. In certain instances, particularly for slab foundations on soft soil, the results can significantly overestimate the velocity of the floor. This overestimation can occur at specific points.

- In the case of a slab on soft soil, an important observation arises. When introducing the phase shift on displacements, it doesn't yield an accurate estimation of the peak caused by the resonance frequency of the soil. This inaccuracy is significant because it impacts the building. The soft soil isn't stiffened by a pile group, making the resonance frequency a key factor.

- For pile group foundations, a noteworthy observation emerges. When the phase shift is incorporated into the base-motion displacements, a comparison is made between the reference solution and the method under study. This comparison reveals a close match between the two.

- In both cases, the presence of coupling terms in the impedance matrix does not affect the results in an appreciable way.

- Applying impedance functions under the building leads to changes in the building's eigenfrequencies and damping. In the case of pile group foundations, the eigenfrequency decreases, whereas in slab foundations, it increases. Regardless of the foundation type, the damping in the structure consistently tends to increase. In pile group foundations, the eigenfrequency decreases while, for the case of slab foundations, it increases. Regardless of the foundation type, the damping in the structure consistently increases.

- The best way to model the phase shift, between the three different approaches that have been tried, is to multiply the amplitude of the displacements of the furter foundations by the cosine of the phase angle.

For a rough analysis, then, the base motion can be applied without taking into count the phase shift; the results will be on the safe side, but overestimate the real velocity of the floors of the building.
If phase shift is introduced, instead, the results will be more precise, except if the velocity of the floors of the building is affected by a peak in frequency at the natural frequency of the soil.
For that frequency interval, is suggested to use the displacements without phase shift and then combine the results.

Appendix A

Appendix A

This Appendix illustrates the floor velocities utilized for investigating the influence of coupling terms in the impedance matrix (Figure A.1 and A.3).
Additionally, it aims to compare the results obtained from different modeling strategies of the phase shift (Figure A.2 and A.4).

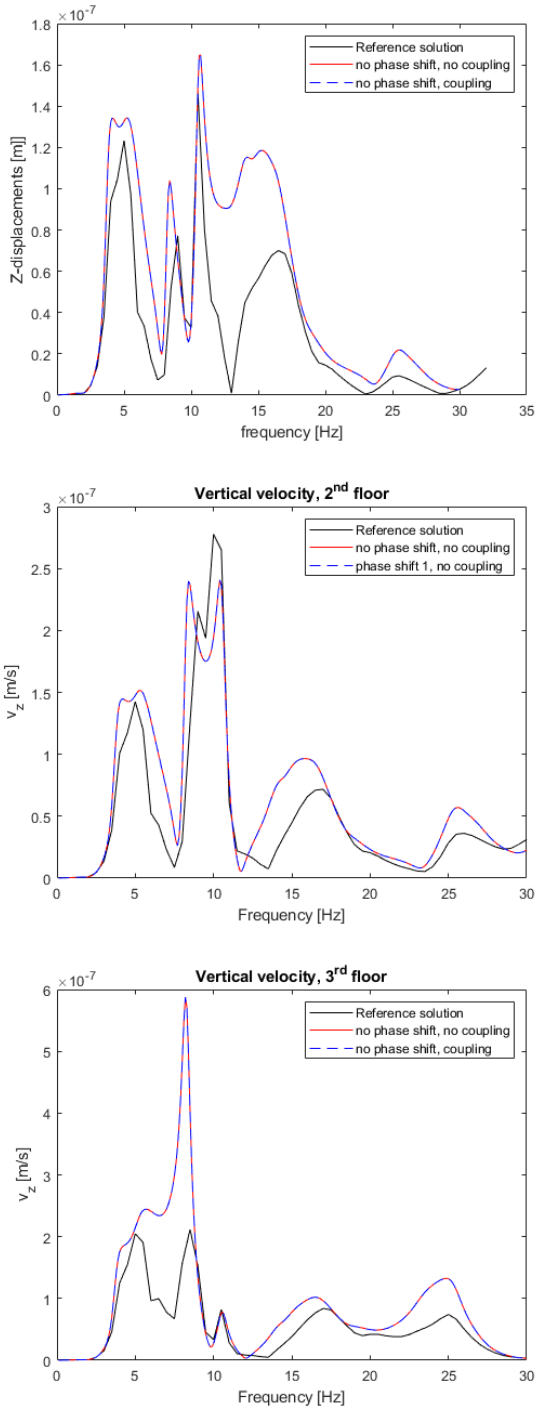

Figure A.1: *Comparison between vertical velocities of the floors of the building obtained from the reference solution (black); by applying a basemotion under the building model with spring and dashpots without a phase shift and without the coupling terms in the impedance matrix (red); by applying a basemotion under the building model with spring and dashpots without a phase shift and with the coupling terms in the impedance matrix (dashed blue); slab foundations.*

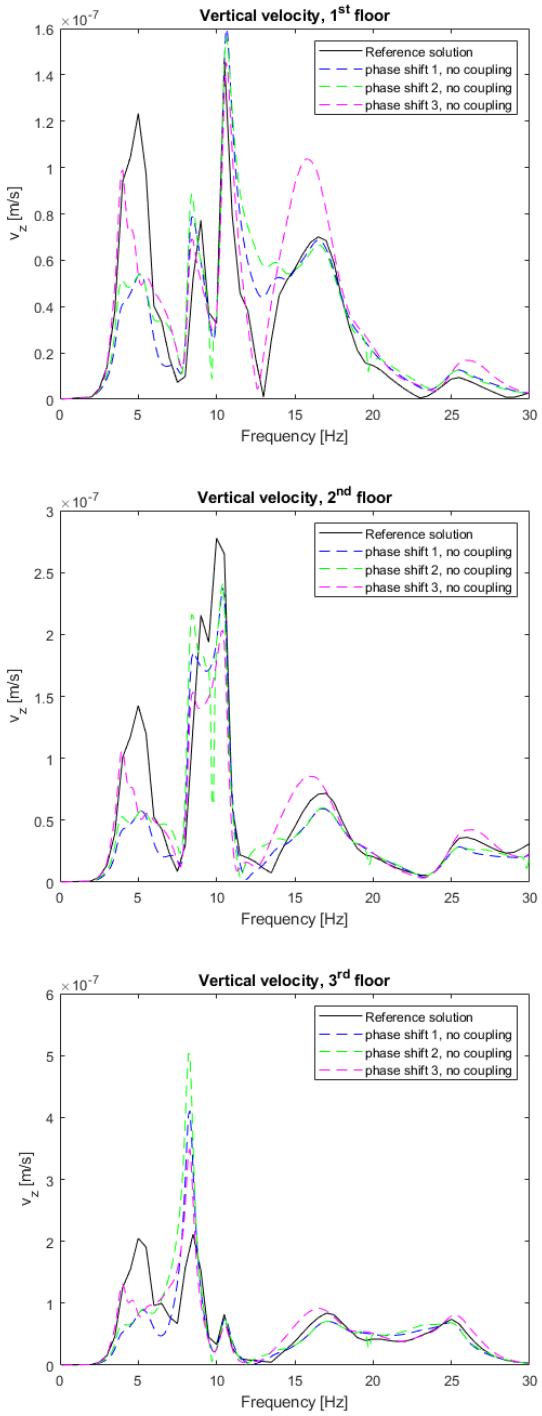

Figure A.2: *Different ways to model the phase shift: reference solution (black); phase shift 1 (blue); phase shift 2 (green); phase shift 3 (purple). For the phase shift modeling approaches refer to subsection 4.3.4; slab foundations.*

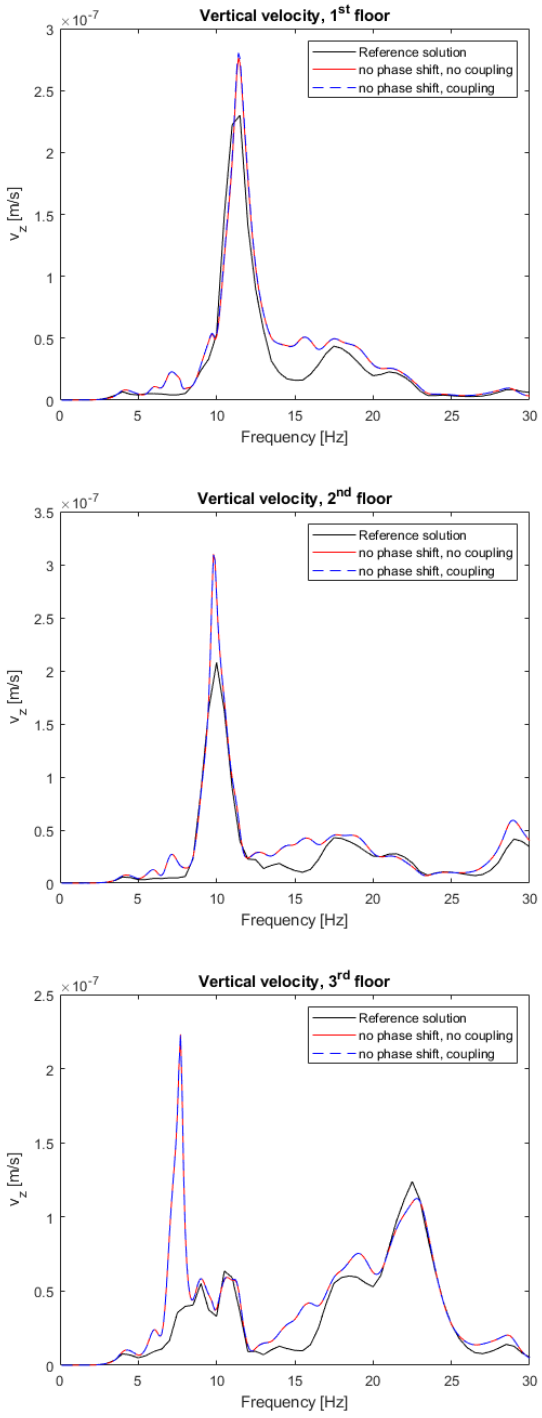

Figure A.3: *Comparison between vertical velocities of the floors of the building obtained from the reference solution (black); by applying a basemotion under the building model with spring and dashpots without a phase shift and without the coupling terms in the impedance matrix (red); by applying a basemotion under the building model with spring and dashpots without a phase shift and with the coupling terms in the impedance matrix (dashed blue); piles group foundations.*

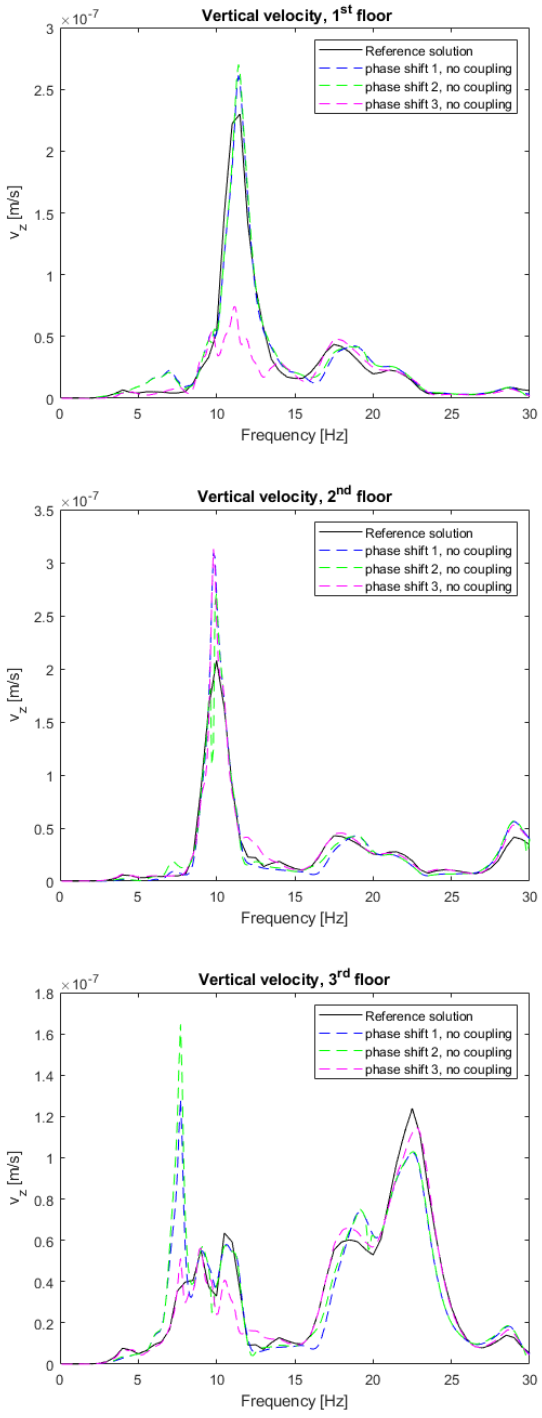

Figure A.4: *Different ways to model the phase shift: reference solution (black); phase shift 1 (blue); phase shift 2 (green); phase shift 3 (purple). For the phase shift modeling approaches refer to subsection 4.3.4; piles group foundations.*

Bibliography

[1] Ricardo Daniel Ambrosini. Material damping vs. radiation damping in soil–structure interaction analysis. *Computers and Geotechnics*, 33(2):86–92, 2006.

[2] GA Athanasopoulos, PC Pelekis, and GA Anagnostopoulos. Effect of soil stiffness in the attenuation of rayleigh-wave motions from field measurements. *Soil Dynamics and Earthquake Engineering*, 19(4):277–288, 2000.

[3] Xuecheng Bian, Hongguang Jiang, Chao Chang, Jing Hu, and Yunmin Chen. Track and ground vibrations generated by high-speed train running on ballastless railway with excitation of vertical track irregularities. *Soil Dynamics and Earthquake Engineering*, 76:29–43, 2015.

[4] Panagiotis Chatzistergos, Sara Behforootan, Roozbeh Naemi, and Nachiappan Chockalingam. Finite element modeling. In *Foot and ankle biomechanics*, pages 365–386. Elsevier, 2023.

[5] Anil K Chopra. *Dynamics of structures*. Pearson Prentice Hall, 2010.

[6] Guillaume Coquel and Corinne Fillol. Analysis of ground-borne noise and vibration levels generated by buses. *Procedia Engineering*, 199:2699–2704, 2017.

[7] Ricardo Dobry and George Gazetas. Dynamic response of arbitrarily shaped foundations. *Journal of geotechnical engineering*, 112(2):109–135, 1986.

[8] Hsai-Yang Fang. *Foundation engineering handbook*. Springer Science & Business Media, 2013.

[9] Zdeněk Kaláb, Markéta Lednická, Robert Kořínek, and Eva Hrubešová. Influence of local geological pattern on values of vibrations induced by road traffic. *Acta Geophysica*, 60:426–437, 2012.

[10] Freddie Karlsson and Abbas Zangeneh. Perfectly matched layers in elastodynamics: Heuristics and comsol implementation. *KTH Royal Institute of Technology, Division of Structural Engineering and Bridges*, 2019.

[11] Victor V Krylov, AR Dawson, ME Heelis, and AC Collop. Rail movement and ground waves caused by high-speed trains approaching track-soil critical velocities. *Proceedings of the Institution of Mechanical Engineers, Part F: Journal of Rail and Rapid Transit*, 214(2):107–116, 2000.

[12] John Lysmer. *Vertical motion of rigid footings*. Number 3. University of Michigan, 1965.

[13] U Nations. Around 2.5 billion more people will be living in cities by 2050, projects new un report. *United Nations https://www. un. org/en/desa/around-25-billion-more-people-will-be-living-cities-2050-projects-new-un-report*, 2018.

[14] LA Padrón, JJ Aznárez, O Maeso, and Masato Saitoh. Impedance functions of end-bearing inclined piles. *Soil dynamics and earthquake engineering*, 38:97–108, 2012.

[15] Manthos Papadopoulos, Stijn François, Geert Degrande, and Geert Lombaert. The influence of uncertain local subsoil conditions on the response of buildings to ground vibration. *Journal of Sound and Vibration*, 418:200–220, 2018.

[16] Karan Kumar Pradhan and Snehashish Chakraverty. Chapter four—finite element method. *Computational structural mechanics*, pages 25–28, 2019.

[17] MG Smith, I Croy, M Ogren, and K Persson Waye. On the influence of freight trains on humans: A laboratory investigation of the impact of nocturnal. 2013.

[18] SIS Swedish Standard. Vibration and shock-method of measurement and guidance levels for the evaluation of comfort in buildings. *SS 460 48 61*, 1992.

[19] John P Wolf. Simple physical models for foundation dynamics. In *Developments in geotechnical engineering*, volume 83, pages 1–70. Elsevier, 1998.

[20] Abbas Zangeneh Kamali. *Dynamic Soil-Structure Interaction Analysis of High-Speed Railway Bridges: Efficient modeling techniques and Experimental testing*. PhD thesis, KTH Royal Institute of Technology, 2021.